nature medicine

Article

https://doi.org/10.1038/s41591-026-04366-x

Low-dose oral nicotinamide mononucleotide for immune thrombocytopenia: a phase 1/2 trial

Received: 25 July 2025

Accepted: 25 March 2026

Published online: 29 April 2026

Check for updates

A list of authors and their affiliations appears at the end of the paper

Autoimmunity remains challenging to treat without broad immunosuppression. We previously showed that anti-CD38 antibody can rapidly elevate platelet counts in refractory immune thrombocytopenia (ITP), but the underlying mechanism was unclear. Here we report that anti-CD38 antibody induces platelet recovery within 3 days, including after retreatment in relapsed cases. Mechanistically, CD38-mediated nicotinamide adenine dinucleotide (NAD^+) depletion drives M1-like macrophage polarization with increased Fc gamma receptor I (FcγRI) expression, thereby promoting macrophage phagocytosis of opsonized platelets. In mice, CD38 inhibition or nicotinamide mononucleotide (NMN) supplementation restores NAD^+, reprograms macrophages, downregulates FcγRI and prevents thrombocytopenia. In an ovalbumin immunization model, NMN treatment does not impair antigen-specific antibody production, supporting preservation of humoral responses. Based on these findings, we conducted a single-arm, open-label phase 1/2 trial of low-dose oral NMN (450 mg twice daily for 2 weeks) in adults with steroid-refractory or steroid-dependent ITP. Primary endpoints were safety/tolerability and platelet response (≥50×10^9 per liter within 2 weeks, confirmed by two consecutive measurements one or more days apart, without rescue therapy or dose escalation of thrombopoietin receptor agonists or corticosteroids). Among 25 enrolled patients, no dose-limiting toxicities or treatment-related serious adverse events occurred; NMN was well tolerated, with only mild treatment-related adverse events in 12% and non-severe infections (grade 1) in 8% of patients while immunoglobulin levels remained stable, consistent with preserved humoral immunity. Five patients (20.0%) met the primary platelet-response endpoint. In exploratory analyses, overall, 60% of patients achieved platelet counts more than 1.5× baseline during treatment, and 52% maintained responses through week 8. Together, these data identify the CD38–NAD^+ axis as an immunometabolic checkpoint in ITP and support further exploration of NMN as a non-antibody-depleting metabolic strategy for antibody-mediated disease. ClinicalTrials.gov identifier: NCT06776510.

e-mail: weijun@ihcams.ac.cn; zhanglei1@ihcams.ac.cn

Autoimmune diseases represent a persistent clinical challenge due to their chronic progression, heterogeneous manifestations, frequent resistance to intervention and limited durability of response. Long-term management primarily depends on broad immunosuppression, which offers limited efficacy and carries cumulative toxicity risks, including increased infection and organ damage[1–3]. Although B-cell-targeted therapies, such as anti-CD20 monoclonal antibodies (mAbs), have improved disease control in certain contexts, their inability to eliminate long-lived plasma cells allows sustained autoantibody production and contributes to disease relapse[4–6]. By contrast, originally developed to target plasma cell malignancies, anti-CD38 mAbs effectively eliminate both short-lived and long-lived plasma cells and have demonstrated promise in refractory autoimmune conditions[7–14]. Immune thrombocytopenia (ITP) is the most common autoantibody-mediated bleeding disorder, characterized by accelerated platelet destruction and impaired thrombopoiesis[3]. Given its well-defined pathophysiology and measurable, rapidly responsive clinical endpoint—platelet count—ITP provides a powerful model for mechanistic dissection and therapeutic exploration of antibody-driven autoimmunity. Our previous studies reported that anti-CD38 mAb treatment was associated with rapid restoration of platelet counts in both adult and pediatric patients with ITP[13,14]. The speed and magnitude of this response suggested additional immunomodulatory mechanisms beyond plasma cell clearance. However, the underlying mechanism remains unclear. In addition, its broader clinical use may be limited by an increased risk of hypogammaglobulinemia and infections, particularly with prolonged exposure[15,16].

Recent advances in immunometabolism have redefined understanding of how metabolic pathways regulate immune cell differentiation, activation and fate decisions. Beyond supporting bioenergetic demands, metabolic flux exerts direct control over immune phenotypes and inflammatory responses[17]. Accordingly, dysregulation of these pathways is central to the pathogenesis of diverse autoimmune diseases, including systemic lupus erythematosus, rheumatoid arthritis and inflammatory bowel disease[18–20]. Consistent with this, conventional agents such as glucocorticoids and methotrexate exert part of their therapeutic effect through metabolic modulation[21–24]. Although experimental models have demonstrated that targeted metabolic reprogramming can suppress pathological immune activity[25–30], efforts to translate these findings into clinical therapies have been limited. CD38, a major nicotinamide adenine dinucleotide (NAD^+) hydrolase upregulated in chronic inflammation and aging, has emerged as an important immunometabolic regulator[31–34]. However, whether its enzymatic activity contributes to immune dysregulation in ITP, and to what extent the rapid therapeutic response to anti-CD38 mAb involves metabolic reprogramming in addition to plasma cell depletion, remains unresolved.

In the present study, we delineate how the CD38–NAD^+ axis may influence macrophage inflammatory programs and platelet clearance in ITP, and we examine whether modulating this pathway can ameliorate thrombocytopenia. We also assess the feasibility of augmenting NAD^+ metabolism with low-dose oral nicotinamide mononucleotide (NMN) in an early-phase clinical setting, with particular attention to preserving humoral immune function, thereby informing a potentially safer approach for longer-term management of antibody-mediated autoimmune cytopenias.

Results

An overview of the experimental datasets, measurements, purposes and key findings corresponding to each figure is provided in Supplementary Table 1.

CD38 blockade rapidly alleviates thrombocytopenia with a major contribution from macrophages

To characterize the temporal dynamics of platelet recovery, high-frequency platelet count monitoring in anti-CD38 mAb-treated patients was carried out and revealed a marked increase in platelet counts within 3 days of infusion, with peak levels by days 6–7 (Fig. 1a and Extended Data Fig. 1a). In three patients who relapsed after an initial response, retreatment with anti-CD38 mAb was associated with renewed platelet recovery within 1 week (Extended Data Fig. 1a,b).

A passive ITP model was established in *Cd38* knockout (*Cd38*KO) mice to delineate the cellular mechanisms underpinning this rapid therapeutic effect (Extended Data Fig. 1c). *Cd38* deficiency significantly ameliorated antiplatelet antibody-induced thrombocytopenia (Fig. 1b and Supplementary Fig. 1), consistent with a role for CD38 in platelet clearance. Bone marrow chimera experiments further showed that the thrombocytopenia-ameliorating effect of *Cd38* deficiency depended on its expression within the hematopoietic compartment (Extended Data Fig. 1d and Supplementary Fig. 2). Lineage-specific depletion indicated that B cells, natural killer cells, $CD4^+$ T cells, $CD8^+$ T cells and neutrophils were dispensable for thrombocytopenia in this passive ITP model (Extended Data Fig. 1e–g and Supplementary Fig. 3). By contrast, macrophage depletion restored platelet counts, and this protective effect was similar between wild-type (WT) and *Cd38*KO mice (Fig. 1c and Supplementary Fig. 1), consistent with CD38-dependent platelet clearance being mediated predominantly through macrophage-intrinsic mechanisms.

Similarly, myeloid-specific *Cd38* deletion ($Cd38^{fl/fl}Lyz2^{iCre+}$) modestly mitigated passive ITP (Extended Data Fig. 1h), consistent with incomplete *Cd38* deletion in splenic macrophages (about 60% deletion efficiency; Supplementary Fig. 4a–c). After macrophage

Fig. 1 | Anti-CD38 mAb therapy rapidly restores platelet counts by suppressing CD38-driven proinflammatory macrophage polarization and platelet clearance in ITP. a, Platelet count kinetics within 14 days after the first anti-CD38 mAb infusion in the retrospective anti-CD38 mAb treatment cohort ($n = 21$). Data are shown as median (IQR). **b**, Daily platelet counts over 7 days after ITP induction in *Cd38*KO and WT mice, with corresponding non-ITP controls (*Cd38*KO-ITP, $n = 10$; *Cd38*KO, $n = 10$; WT-ITP, $n = 9$; WT, $n = 9$). **c**, Daily platelet counts after ITP induction in mice treated with clodronate liposomes (macrophage depletion) or control liposomes (WT+clodronate, $n = 10$; *Cd38*KO+clodronate, $n = 10$; WT+control, $n = 10$). **d**, Representative immunofluorescence (IF) images of splenic M1 ($DAPI^+F4/80^+iNOS^+$) and M2 ($DAPI^+F4/80^+CD163^+$) macrophages in WT and *Cd38*KO mice with or without ITP induction. Scale bars, 20 µm. **e**, Quantification of splenic M1/M2 macrophage ratio in WT and *Cd38*KO mice with or without ITP assessed by IF staining ($n = 6$ per group). **f**, Circulating persistence of transfused fluorescently labeled opsonized platelets in WT and *Cd38*KO mice at indicated timepoints ($n = 7$ per group). **g**, Workflow for spleen sample collection and downstream analysis from splenectomized patients with ITP and trauma controls. **h**, Representative IF images showing M1 ($DAPI^+CD68^+iNOS^+$) and M2 ($DAPI^+CD68^+CD163^+$) macrophages, together with CD38 distribution, in spleens from patients with ITP and trauma controls. Scale bars, 20 µm. **i**, Frequency of splenic M1 macrophages in spleens from patients with ITP ($n = 18$) and trauma controls ($n = 7$) assessed by IF staining. **j**, Workflow for multidimensional profiling of peripheral blood from patients with ITP before and after anti-CD38 mAb therapy. PBMCs were collected at day 0 and day 56 for scRNA-seq; plasma was collected at day 0 and day 8 for Olink profiling. **k**, M1 gene signature scores in classical monocytes from normal controls (NC, $n = 6$), relapsed patients ($n = 4$) and sustained responders ($n = 5$) before and after anti-CD38 mAb therapy. Data are shown as median (IQR). **l**, Plasma arginase 1 (ARG1) levels in sustained responders before and after anti-CD38 mAb treatment ($n = 14$). Unless otherwise stated, data are presented as mean ± s.e.m. Statistical differences were determined by two-way repeated-measures ANOVA for prespecified pairwise comparisons (**b**,**c**), two-sided Mann–Whitney *U*-tests for prespecified pairwise comparisons (**e**,**f**,**i**,**k**) or two-sided Wilcoxon signed-rank test (**l**). Absence of *P* value indicates that no comparison was performed. D, day; h, hour; ITPSP, spleen from patients with ITP; NCSP, spleen from trauma controls; SP, spleen; SPMC, splenic mononuclear cell. Panels **g** and **j** created in BioRender: **g**, Li, H. https://biorender.com/v8moe93 (2026); **j**, Li, H. https://biorender.com/w17bfbc (2026).

https://doi.org/10.1038/s41591-026-04366-x

depletion, *Cd38*KO (versus WT) bone marrow-derived macrophages (BMDMs) transfer also mitigated anti-CD41-induced thrombocytopenia (Supplementary Fig. 4d), supporting a macrophage-intrinsic role for CD38 in platelet clearance.

CD38 drives proinflammatory macrophage polarization and platelet destruction in ITP

To assess whether CD38 influences macrophage abundance or effector state in ITP, we profiled splenic macrophages in WT-ITP and *Cd38*KO-ITP mice. Splenic macrophage counts were equivalent between WT-ITP and *Cd38*KO-ITP mice (Extended Data Fig. 2a), whereas CD38 inhibition (78c) in BMDMs reduced M1-associated transcriptional programs and increased M2-related transcriptional signatures (Extended Data Fig. 2b–j). Consistently, immunofluorescence staining confirmed an increased splenic M1/M2 macrophage ratio in WT-ITP mice compared to *Cd38*KO-ITP mice (Fig. 1d,e and Extended Data Fig. 3a,b), consistent with the flow cytometry findings (Extended Data Fig. 3c–e). Functionally, *Cd38* deficiency impaired the clearance of transfused, fluorescently labeled and opsonized platelets in vivo (Fig. 1f and Extended Data Fig. 3f). In vitro, low-dose lipopolysaccharide (LPS) stimulation of *Cd38*KO BMDMs exhibited elevated M2 polarization, along with a reduced M1/M2 ratio, markedly lower

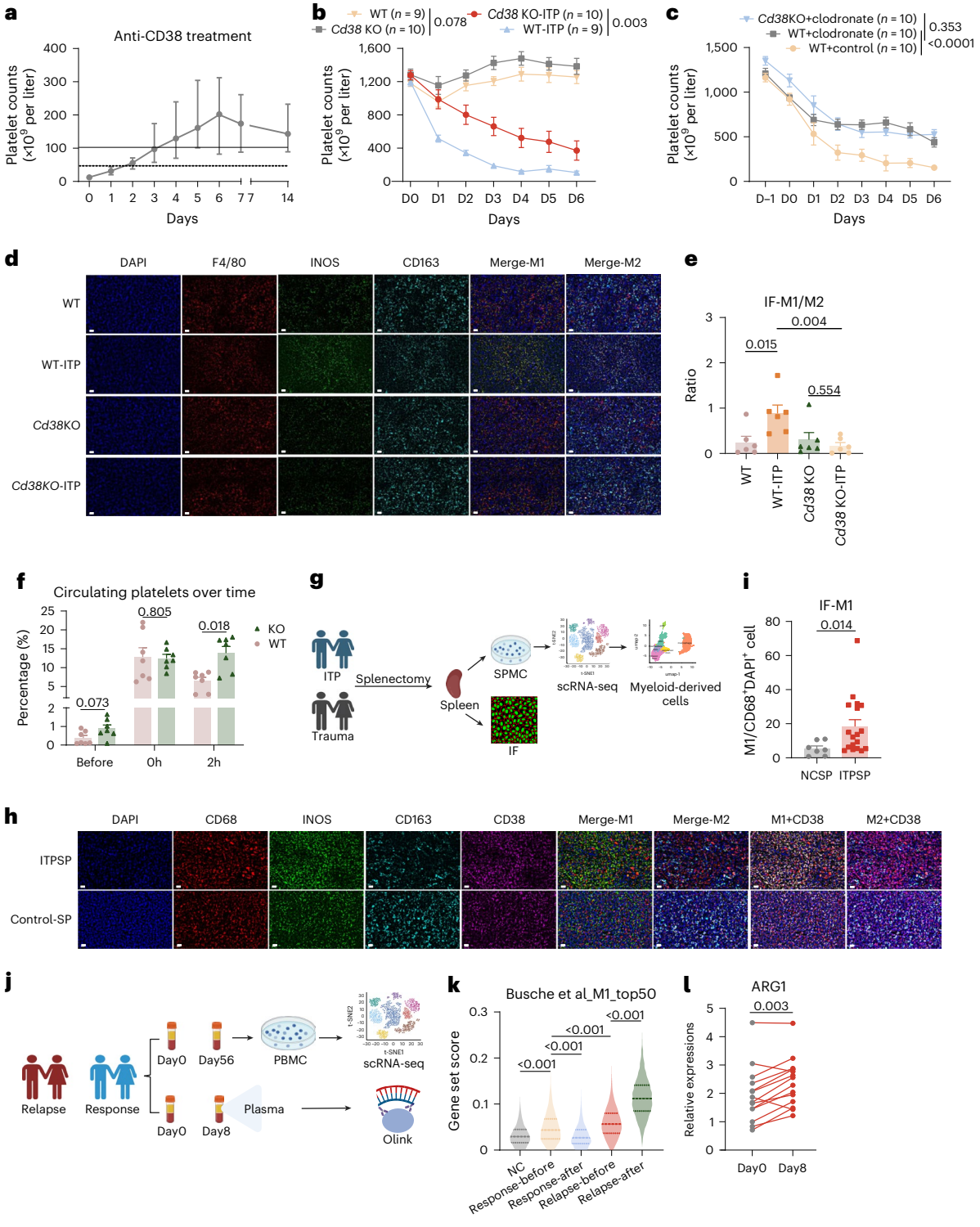

surface Fc gamma receptor I (FcγRI) expression and lower expression of TNF and IL-6 compared to WT BMDMs (Extended Data Fig. 3g–k). Collectively, these results further implicate CD38 in promoting inflammatory macrophage polarization and platelet clearance.

To determine whether these observations are recapitulated in patients, spleen tissue from patients with ITP and trauma splenectomy controls was analyzed (Fig. 1g). Immunofluorescence analysis demonstrated an enrichment of M1-polarized macrophages in ITP samples, along with an elevated trend in the M1/M2 ratio (Fig. 1h,i and Extended Data Fig. 4a,b). In addition, CD38 expression was elevated in M1 macrophages as compared to M2 macrophages in the spleen of patients with ITP (Extended Data Fig. 4c). Complementary single-cell RNA sequencing (scRNA-seq) of splenic myeloid populations suggests a modest but directionally consistent shift toward an M1-associated transcriptional program in ITP macrophages (Extended Data Fig. 4d–i). These results, as supportive evidence for the immunofluorescence findings, indicate a proinflammatory skewing of splenic macrophages in ITP that may be permissive for enhanced Fcγ receptor-dependent platelet clearance and disruption of megakaryopoiesis[35–37]. Additionally, CD38 transcript levels were elevated in ITP macrophages (Extended Data Fig. 4j,k). To further address the link between CD38-targeted therapy and macrophage phenotype in patients, longitudinal scRNA-seq and protein profiling were performed in peripheral blood mononuclear cells (PBMCs) and plasma from patients with ITP receiving anti-CD38 mAb treatment (Fig. 1j). Reduced M1-like gene expression was observed in classical monocytes from sustained responders over time, whereas non-responders exhibited no similar transcriptional reprogramming (Fig. 1k, Extended Data Fig. 4l,m and Supplementary Fig. 5). Proteomic analysis of matched plasma samples further showed increased levels of arginase 1, a canonical M2 marker, after treatment in sustained responders (Fig. 1l). Together, these results reveal that patients with ITP exhibit a polarization bias toward proinflammatory M1 macrophages, which can be corrected by anti-CD38 mAb treatment.

CD38–NAD$^+$ axis regulates macrophage polarization and autoantibody-mediated platelet destruction

Given the role of CD38 in NAD$^+$ metabolism, we examined whether CD38-mediated NAD$^+$ depletion is associated with proinflammatory macrophage polarization in ITP. Gene set enrichment scoring of single-cell transcriptomes from classical monocytes before and after anti-CD38 mAb treatment revealed reduced expression of NAD$^+$ metabolism-associated gene signatures in sustained responders (Fig. 2a), implicating CD38-dependent NAD$^+$ catabolism in shaping macrophage polarization. In support of this, BMDMs derived from *Cd38*KO mice displayed significantly higher intracellular levels of both NAD$^+$ and NADH under LPS stimulation, accompanied by an increased NAD$^+$/NADH ratio relative to WT controls (Fig. 2b and Extended Data Fig. 5a,b). Supplementation with the NAD$^+$ precursor NMN similarly enhanced intracellular NAD$^+$, NADH levels and NAD$^+$/NADH ratio in BMDMs (Fig. 2c and Extended Data Fig. 5c,d). NMN also reduced M1 polarization and the M1/M2 macrophage ratio (Fig. 2d and Extended Data Fig. 5e–g); dampened M1-associated effector programs, including decreased expression of FcγRI and reduced production of M1-associated markers including iNOS and TNF (Fig. 2e and Extended Data Fig. 5h,i); and attenuated phagocytosis of opsonized platelets (Fig. 2f).

To further explore the underlying molecular basis, transcriptional analyses were performed. NMN treatment downregulated NF-κB signaling (Fig. 2g), supported by reduced phosphorylation of NF-κB p65 in NMN-treated BMDMs (Fig. 2h). Mechanistically, NF-κB modulation by betulinic acid abolished NMN-induced inhibition of M1 polarization (Fig. 2i and Extended Data Fig. 5j,k), indicating that NAD$^+$ exerts antiinflammatory effects, at least in part, through suppression of NF-κB signaling in macrophages[38–41]. NMN was also associated with reduced NOD-like receptor thermal protein domain-associated protein 3 (NLRP3) inflammasome priming and activation, as shown by reduced NLRP3 protein abundance in LPS-primed BMDMs, decreased caspase-1 activity upon nigericin challenge and lower IL-1β levels in culture supernatants (Extended Data Fig. 5l–n). Together, these findings reveal that restoration of intracellular NAD$^+$ in macrophages reverses inflammatory activation and attenuates platelet phagocytosis in association with suppression of NF-κB signaling and NLRP3 inflammasome activation.

To assess the therapeutic relevance in vivo, NMN was administered to mice with antibody-induced passive ITP, with the selective CD38 inhibitor 78c as a pharmacologic benchmark. Both interventions increased platelet counts without altering total splenic macrophage abundance (Fig. 2j, Extended Data Fig. 5o,p and Supplementary Fig. 6). Immunofluorescence imaging and flow cytometry revealed a lower M1/M2 ratio after treatment (Fig. 2k–m and Extended Data Fig. 5q–t), indicative of a shift toward a less inflammatory tissue environment. In addition, NAD$^+$ augmentation did not alter plasma cell frequency (Fig. 2n), and serum immunoglobulin levels remained stable (Fig. 2o and Extended Data Fig. 5u,v). To directly assess antigen-specific humoral immunity, we further performed an ovalbumin (OVA) immunization model under ongoing NMN treatment. NMN did not alter the frequency of splenic germinal center B (GCB) cells at the endpoint nor did it affect

Fig. 2 | CD38 regulates macrophage polarization via NAD$^+$ metabolism, and NMN reverses macrophage polarization and ameliorates thrombocytopenia. **a**, Gene set scores of NAD$^+$ metabolic pathway in classical monocytes from normal controls (NC, $n = 6$), relapsed patients ($n = 4$) and sustained responders ($n = 5$) before and after anti-CD38 mAb therapy. Data are shown as median (IQR). **b**, Intracellular NAD$^+$ levels in BMDMs from WT versus *Cd38*KO mice after LPS stimulation ($n = 6$ per group). **c**, Intracellular NAD$^+$ levels in BMDMs with or without NMN supplementation after LPS stimulation ($n = 10$ per group). **d**, M1/M2 polarization ratio in BMDMs with or without NMN supplementation after LPS stimulation ($n = 6$ per group). **e**, Expression levels of FcγRI on BMDMs with or without NMN supplementation after LPS stimulation, quantified as mean fluorescence intensity (MFI) ($n = 14$ per group). **f**, Phagocytic Index of BMDMs toward opsonized platelets with or without NMN supplementation after LPS stimulation ($n = 10$ per group). **g**, GSEA of the canonical NF-κB signaling pathway based on RNA-seq profiles of BMDMs treated with or without NMN ($n = 4$ per group). **h**, Immunoblot analysis of total and phosphorylated NF-κB p65 in BMDMs pretreated with NMN (2 hours) or vehicle, followed by betulinic acid (BA, NF-κB modulator) or vehicle for 30 minutes and then LPS stimulation for 30 minutes. **i**, M1/M2 macrophage ratio assessed by flow cytometry in BMDMs after LPS stimulation under control, NMN or NMN+BA treatment conditions ($n = 10$ per group). **j**, Daily platelet count kinetics in passive ITP mice treated with NMN ($n = 11$), CD38 inhibitor 78c ($n = 6$) or vehicle control ($n = 10$). **k**, Representative IF images of splenic macrophage subsets (M1: DAPI$^+$F4/80$^+$iNOS$^+$; M2: DAPI$^+$F4/80$^+$CD163$^+$) in ITP mice treated with NMN, 78c or vehicle control. Scale bars, 20 μm. **l**,**m**, Splenic M1/M2 macrophage ratio in ITP mice treated with NMN, 78c or vehicle control detected by IF staining (**l**) ($n = 5$ per group) and flow cytometry (**m**) ($n = 21$ for control, $n = 23$ for NMN, $n = 9$ for 78c). **n**, Percentages of splenic plasma B cells (CD19$^+$IgD$^-$CD138$^+$) among total B cells (CD19$^+$) analyzed by flow cytometry in ITP mice treated with NMN, 78c or vehicle control ($n = 6$ per group). **o**, Plasma IgG concentrations in ITP mice treated with NMN ($n = 11$), 78c ($n = 10$) or vehicle control ($n = 11$). **p**, Percentages of splenic GCBs in OVA/alum-immunized BALB/c mice treated with NMN or vehicle control at day 21 after immunization ($n = 9$ per group). **q**,**r**, OVA-specific IgG (**q**) and IgM (**r**) responses in OVA/alum-immunized BALB/c mice treated with NMN or vehicle control at the indicated timepoints after immunization ($n = 10$ per group). Unless otherwise stated, data are presented as mean ± s.e.m. Statistical differences were determined by two-sided Mann–Whitney *U*-tests for prespecified pairwise comparisons (**a**,**b**,**l**–**r**), two-way repeated-measures ANOVA for prespecified pairwise comparisons (**j**) or two-sided Wilcoxon signed-rank tests (**c**–**f**,**i**). Absence of *P* value indicates that no comparison was performed. D, day; NES, normalized enrichment score.

https://doi.org/10.1038/s41591-026-04366-x

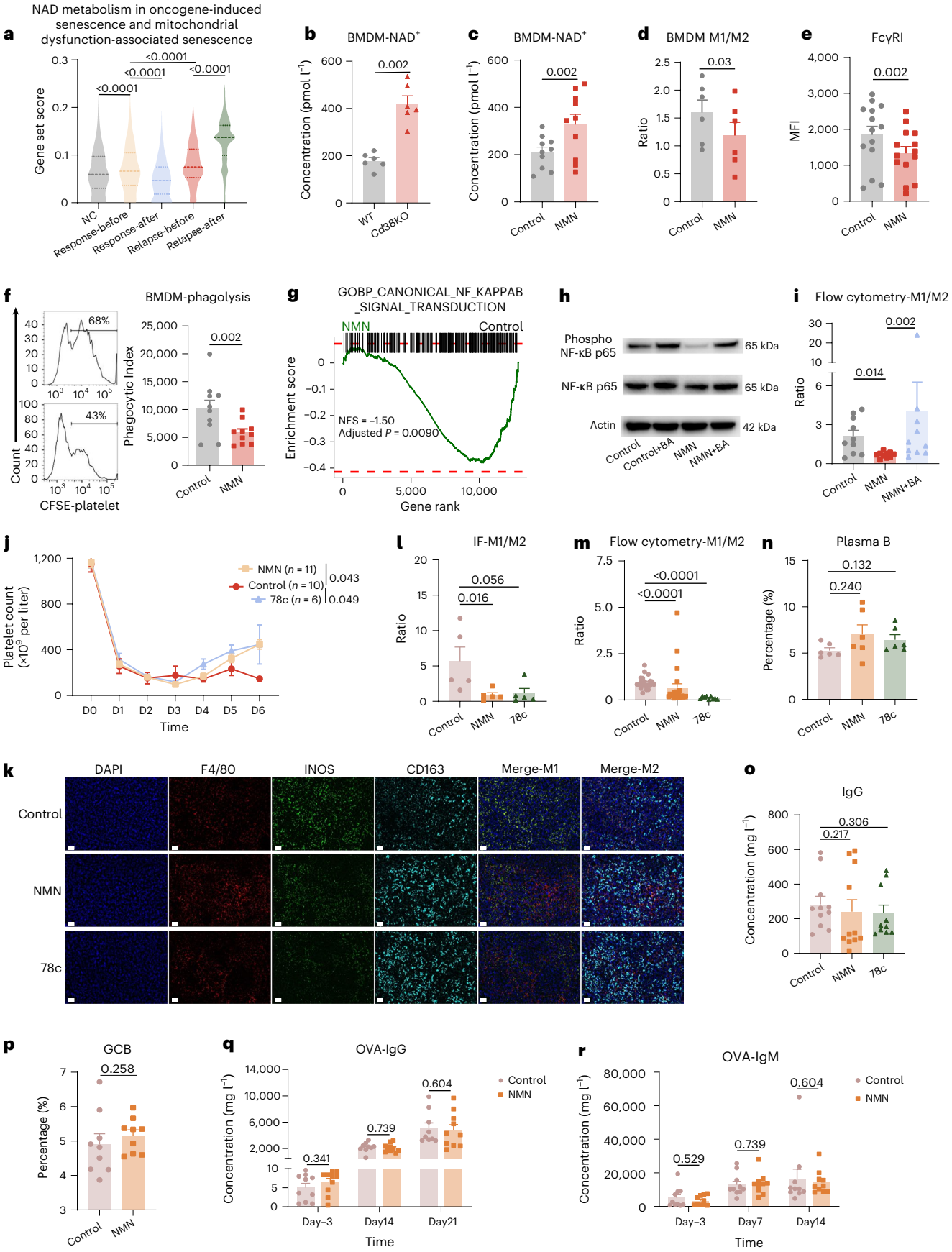

https://doi.org/10.1038/s41591-026-04366-x

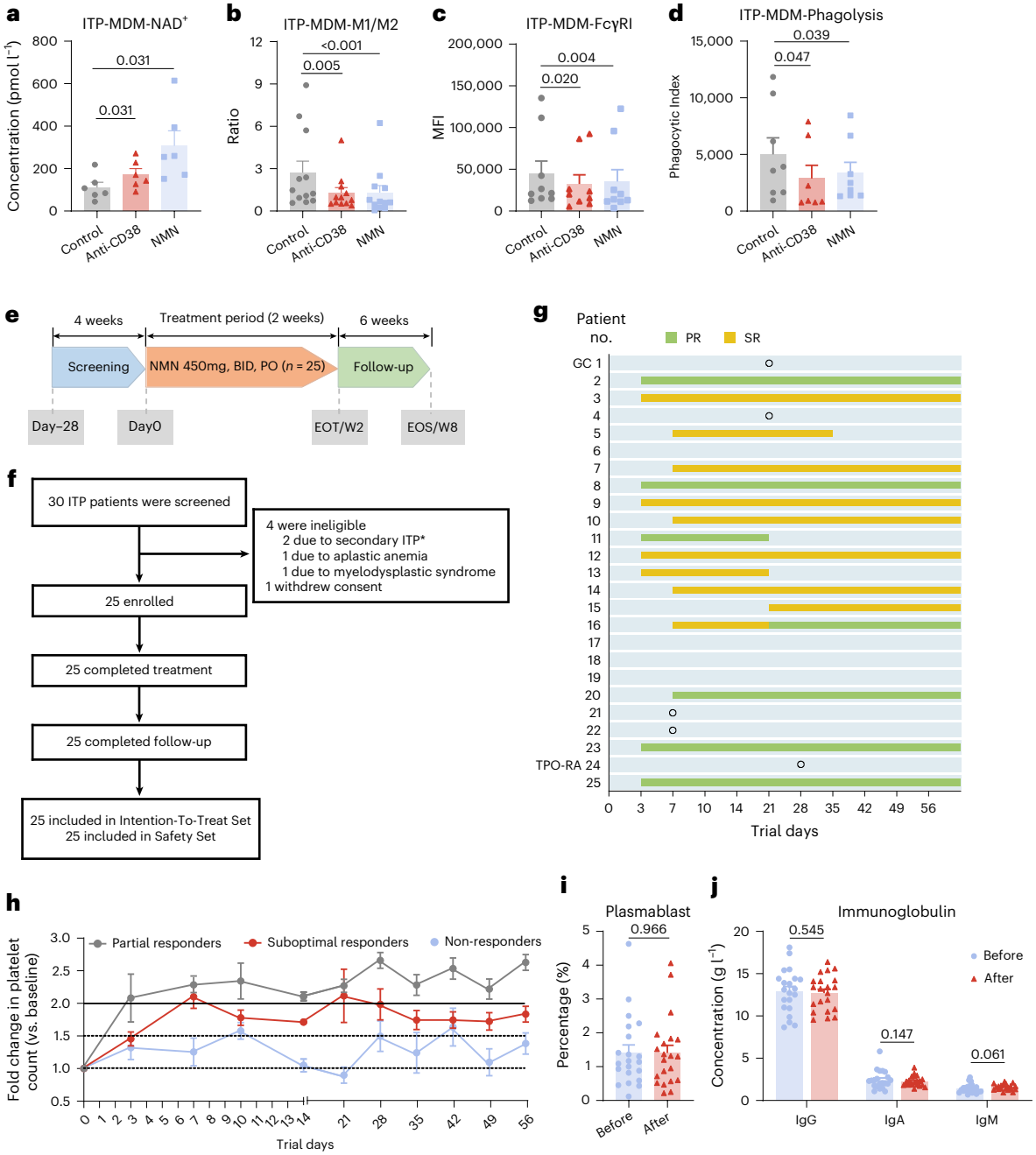

Fig. 3 | Oral NMN therapy rapidly improves platelet counts in patients with ITP. **a**, Intracellular NAD^+ levels in MDMs from patients with ITP after ex vivo treatment with anti-CD38 mAb, NMN or vehicle control ($n = 6$). **b**, M1/M2 macrophage ratio in MDMs from patients with ITP after ex vivo treatment with anti-CD38 mAb, NMN or vehicle control ($n = 12$). **c**, Expression levels of FcγRI on MDMs from patients with ITP after ex vivo treatment with anti-CD38 mAb, NMN or vehicle control ($n = 9$). **d**, Phagocytosis Index of opsonized platelets by MDMs from patients with ITP after ex vivo treatment with anti-CD38 mAb, NMN or vehicle control ($n = 8$). **e**,**f**, Study design (**e**) and enrollment summary (**f**) for the open-label, single-arm phase 1/2 clinical trial of low-dose oral NMN in ITP. *Secondary ITP included systemic lupus erythematosus ($n = 1$) and common variable immunodeficiency disease ($n = 1$). **g**, Swimmer plot showing individual patient responses over trial days. Response categories (non-response, partial response (PR) and suboptimal response (SR)) were assigned according to the prespecified criteria described in Methods; circles indicate rescue therapy. Concomitant medications are labeled on the left (GC, glucocorticoids). **h**, Fold change in platelet count relative to baseline over trial days in partial responders ($n = 6$), suboptimal responders ($n = 9$) and non-responders ($n = 10$) according to the efficacy status on day 14. **i**, Frequency of plasmablasts ($CD19^+CD27^+CD138^+$) among total B cells ($CD19^+$) before and 8 weeks after NMN treatment, assessed by flow cytometry ($n = 21$). **j**, Serum immunoglobulin (IgG, IgA and IgM) concentrations in patients with ITP before and 8 weeks after NMN treatment ($n = 21$). Unless otherwise stated, data are presented as mean ± s.e.m. Statistical differences were determined by two-sided Wilcoxon signed-rank tests (**a**–**d**,**i**,**j**). Absence of *P* value indicates that no comparison was performed. BID, twice daily; EOS, end of study; EOT, end of treatment; MFI, mean fluorescence intensity; PO, oral; W, week.

OVA-specific IgG or IgM responses over time, compared to vehicle controls (Fig. 2p–r). These results suggest that NMN supplementation alleviates thrombocytopenia while preserving humoral immune integrity in the preclinical model.

Oral NMN administration achieves high safety and rapid efficacy in patients with ITP

To bridge this translational gap and evaluate whether NAD^+ supplementation could similarly modulate macrophage function and alleviate

https://doi.org/10.1038/s41591-026-04366-x

Table 1 | Baseline characteristics of enrolled patients in the NMN-treated ITP clinical registry study

Characteristic	NMN treated (*n*=25)
Sex, *n* (%)	
Male	5 (20.0)
Female	20 (80.0)
Median (IQR) age, years	43.0 (32.0–54.5)
Median (IQR) BMI, kg m^{-2}	24.6 (21.2–27.8)
Median (IQR) duration of ITP, months	36.0 (21.5–73.5)
ITP phases	
Persistent	2 (8.0)
Chronic	23 (92.0)
Median (IQR) baseline platelet count, ×10^9 per liter	23.0 (19.5–26.0)
Baseline platelet count, *n* (%)	
<20×10^9 per liter	6 (24.0)
20–30×10^9 per liter	19 (76.0)
Previous ITP therapy, *n* (%)	
Glucocorticoids	25(100.0)
IVIG	5 (20.0)
rhTPO	2 (8.0)
TPO-RA	4 (16.0)
RTX	0 (0)
Danazol	2 (8.0)
Cyclosporine	1 (4.0)

BMI, body mass index; rhTPO, recombinant human thrombopoietin; RTX, rituximab.

Table 2 | Efficacy of oral NMN in adults with ITP

	NMN (*n*=25)
Primary endpoints	
Proportion of patients with two or more consecutive PLT ≥ 50×10^9 per liter within 2 weeks	5 (20.0)
Secondary endpoints	
PR rate within 4 weeks	7 (28.0)
PR rate at week 2	6 (24.0)
PR rate at week 4	6 (24.0)
PR rate at week 8	6 (24.0)
SR rate at week 2	9 (36.0)
SR rate at week 4	8 (32.0)
SR rate at week 8	7 (28.0)
Proportion of patients with PLT ≥ 50×10^9 per liter at week 2	2 (8.0)
Proportion of patients with PLT ≥ 50×10^9 per liter at week 4	6 (24.0)
Proportion of patients with PLT ≥ 50×10^9 per liter at week 8	6 (24.0)
Proportion of patients with PLT ≥ 50×10^9 per liter within 4 weeks	13 (52.0)
Time to PLT ≥ 30×10^9 per liter (at least 2× from baseline PLT), weeks, median (IQR)[a]	1.0 (1.0–1.0)
Time to PLT ≥ 50×10^9 per liter, weeks, median (IQR)[b]	1.0 (1.0–1.0)
Cumulative duration of PLT ≥ 30×10^9 per liter (at least 2× from baseline) within 8 weeks, weeks, median (IQR)[c]	7.0 (5.0–7.0)
Cumulative duration of PLT ≥ 50×10^9 per liter within 8 weeks, weeks, median (IQR)[d]	6.0 (3.5–6.5)

Data are presented as median (IQR) or *n* (%). Partial response (PR) was defined as at least two consecutive (separated by ≥7 days) PLT ≥ 30×10^9 per liter but <100×10^9 per liter, with a minimum doubling from baseline, in the absence of bleeding; suboptimal response (SR) was defined as PLT ≥ 30×10^9 per liter with a ≥1.5-fold but <2-fold increase from baseline and no bleeding, confirmed by at least two PLT measurements taken at least 7 days apart. [a]Time to PLT ≥ 30×10^9 per liter (≥2-fold increase from baseline) was defined as the time to the first of two consecutive PLT ≥ 30×10^9 per liter (≥2-fold increase from baseline, separated by ≥7 days) without having received any platelet-elevating therapy or having had a dose increment of TPO-RAs and/or corticosteroids. [b]Time to PLT ≥ 50×10^9 per liter was defined as the time to the first two consecutive PLT ≥ 50×10^9 per liter (separated by ≥7 days) without having received any PLT-elevating therapy or having had a dose increment of TPO-RAs and/or corticosteroids. [c]Defined as the cumulative time from the first two consecutive PLT ≥ 30×10^9 per liter and at least doubled from baseline to the first two consecutive PLT < 30×10^9 per liter or lower than double from baseline or up to week 8, whichever occurred first. [d]Defined as the cumulative time from the first two consecutive PLT ≥ 50×10^9 per liter to the first two consecutive PLT < 50×10^9 per liter or up to week 8, whichever occurred first. PLT, platelet count.

platelet destruction in humans, monocyte-derived macrophages (MDMs) from patients with ITP and normal controls were treated with NMN. NMN increased intracellular NAD^+ levels, decreased the M1/M2 ratio, downregulated FcγRI expression and suppressed phagocytosis of opsonized platelets (Fig. 3a–d and Extended Data Fig. 6a–j), consistent with the macrophage-reprogramming effects observed in the preclinical models.

Based on these mechanistic data and prior safety data for NMN in human studies[42–45], a single-arm, open-label phase 1/2 clinical trial was initiated to evaluate low-dose oral NMN monotherapy in adults with primary ITP who had failed to achieve or maintain a response after corticosteroid therapy and either had prior failure of second-line treatments or could not access them for financial reasons (ClinicalTrials.gov identifier: NCT06776510). Key inclusion criteria were age ≥18 years; ITP duration ≥3 months; platelet count <30 × 10^9 per liter within 2 days prior to enrollment, confirmed by two or more measurements at least 1 day apart; and Eastern Cooperative Oncology Group (ECOG) performance status ≤2. Patients receiving stable maintenance therapy were eligible, provided they were receiving no more than one concomitant agent (corticosteroids ≤0.5 mg kg^{-1} prednisone-equivalent or a TPO receptor agonist (TPO-RA)) at a stable dose for ≥4 weeks before the first NMN dose; dose escalation of these agents and new platelet-elevating therapies were not allowed during the study, unless rescue/emergency intervention was clinically required.

The trial had two prespecified primary endpoints: (1) safety and tolerability, assessed by the incidence and severity of treatment-emergent adverse events and serious adverse events (SAEs) graded by National Cancer Institute Common Terminology Criteria for Adverse Events (NCI-CTCAE) version 5.0, together with protocol-specified routine laboratory tests; and (2) efficacy, defined as the proportion of patients achieving a platelet count ≥50 × 10^9 per liter within 2 weeks of treatment initiation (two consecutive measurements at least 1 day apart), in the absence of rescue therapy and without dose escalation of TPO-RAs or corticosteroids. Prespecified secondary endpoints included (1) the proportion of patients with platelet count ≥50 × 10^9 per liter at each scheduled visit (weeks 1, 2, 3, 4, 6 and 8); (2) time to platelet count ≥30 × 10^9 per liter (with at least a two-fold increase from baseline) and to ≥50 × 10^9 per liter; (3) platelet counts at each scheduled visit; (4) the proportion of patients receiving emergency (rescue) treatment within 2 weeks and over the entire study period; (5) cumulative weeks with platelet count ≥30 × 10^9 per liter and ≥50 × 10^9 per liter during the 8-week study period; (6) change in bleeding score from baseline to week 2 assessed by the World Health Organization (WHO) Bleeding Scale; (7) the proportion of patients achieving platelet counts ≥50 × 10^9 per liter at least once within the first 4 weeks; (8) partial response rate within 4 weeks; and (9) the proportion of suboptimal response at each scheduled visit. Definitions of partial response and suboptimal response are provided in the 'Response definitions' subsection of Methods. Not all prespecified secondary endpoints are fully reported in this paper: for secondary endpoint (1) (proportion of patients with platelet count ≥50 × 10^9 per liter) and secondary endpoint (9) (evaluation of suboptimal response at each visit period), we selectively reported clinically relevant timepoints (weeks 2, 4 and 8) to maintain readability and avoid

https://doi.org/10.1038/s41591-026-04366-x

Table 3 | Adverse events in patients with ITP treated with oral NMN

Adverse event	Patients (n=25)				
	Grade 1	Grade 2	Grade 3	Grade 4 or 5	Any grade
	Number of patients (percent)				
Asthenia	1 (4)	0 (0)	0 (0)	0 (0)	1 (4)
Nausea	1 (4)	0 (0)	0 (0)	0 (0)	1 (4)
Vomiting	1 (4)	0 (0)	0 (0)	0 (0)	1 (4)
Headache	1 (4)	0 (0)	0 (0)	0 (0)	1 (4)
Upper respiratory tract infection	1 (4)	0 (0)	0 (0)	0 (0)	1 (4)
Oral herpes	1 (4)	0 (0)	0 (0)	0 (0)	1 (4)

redundancy. We think that these timepoints are representative and are sufficient to demonstrate treatment efficacy. Further details of the trial are provided in Supplementary Information.

A total of 30 patients were screened. Twenty-five were enrolled between 15 January and 17 March 2025. All patients received oral NMN at a dose of 450 mg twice daily for 2 weeks, followed by a 6-week observation period (Fig. 3e,f). Baseline characteristics are summarized in Table 1. The median age was 43.0 years (interquartile range (IQR), 32.0–54.5), and 80% (20/25) were female. The median duration of ITP was 36.0 months (IQR, 21.5–73.5), with most patients (92%) classified as having chronic ITP. The median baseline platelet count was 23.0×10^9 per liter (IQR, 19.5–26.0). All patients had previously received glucocorticoid therapy, and 20% had received intravenous immunoglobulin (IVIG). Use of recombinant human thrombopoietin and TPO-RAs was reported in 8% and 16% of patients, respectively.

Five of 25 patients (20.0%) met the primary efficacy endpoint. Among key secondary endpoints, the median time to achieve platelet counts $\geq 30 \times 10^9$ per liter (with at least a two-fold increase from baseline) was 1.0 weeks (IQR, 1.0–1.0; $n = 7$), and the median time to reach $\geq 50 \times 10^9$ per liter was also 1.0 weeks (IQR, 1.0–1.0; $n = 3$), mirroring the rapid response kinetics previously observed with anti-CD38 mAb therapy. Platelet counts increased rapidly and were maintained throughout the 8-week follow-up (Fig. 3g, Extended Data Fig. 6k and Supplementary Table 2). The median cumulative duration of platelet counts $\geq 30 \times 10^9$ per liter within the 8-week period was 7.0 weeks (IQR, 5.0–7.0; $n = 7$), and the cumulative duration of platelet counts $\geq 50 \times 10^9$ per liter was 6.0 weeks (IQR, 3.5–6.5; $n = 3$). The detailed efficacy outcomes, including primary and secondary endpoints, are listed in Table 2. Accordingly, the WHO bleeding score was slightly decreased in the enrolled patients (Extended Data Table 1 and Supplementary Table 3). Six patients (24.0%) achieved a partial response by week 2, and this proportion remained stable at week 4 and week 8 (6/25, 24.0%). Suboptimal response was observed in 36.0%, 32.0% and 28.0% of patients at weeks 2, 4 and 8, respectively (Extended Data Fig. 6l). Platelet count trajectories over the 8-week follow-up differed according to week 2 response category (Fig. 3h). By week 8, 13 of 25 patients (52.0%) remained in either partial response ($n = 6$) or suboptimal response ($n = 7$), despite the intentionally conservative dosing regimen employed for safety.

The treatment was well tolerated, with only mild adverse events observed in the NMN trial. Overall, three of 25 patients (12%) experienced treatment-emergent adverse events, all of which were grade 1: one patient developed an upper respiratory tract infection; one patient reported asthenia accompanied by oral herpes; and one patient experienced headache with nausea and vomiting. No grade 2 or higher events, dose-limiting toxicities or treatment-related SAEs occurred (Table 3). All treatment-emergent adverse events captured by the protocol-specified safety assessments are summarized above, and no additional adverse events were recorded. Longitudinal hematologic monitoring showed no significant changes in total leukocyte counts or differential cell counts during NMN treatment and follow-up (Supplementary Table 4). For infection-related safety, we focused on grade 2 or higher infections: no patient in the NMN group developed a grade 2 or higher infection, whereas, in the retrospective anti-CD38 mAb cohort, four of 21 patients (19.0%) experienced grade 2 upper respiratory tract infections (Extended Data Table 2). Any-grade infections were reported descriptively to facilitate cross-cohort comparison: in the NMN trial, only two of 25 patients (8%) had grade 1 infections (one upper respiratory tract infection and one oral herpes) compared to nine of 21 patients (42.9%) with any-grade infection (including grade 1 upper respiratory tract infections, grade 1 neutropenia and grade 2 upper respiratory tract infections) in the anti-CD38 mAb cohort. Nonetheless, these cross-cohort comparisons should be interpreted descriptively, given the non-head-to-head nature of the cohorts and differences in ascertainment/reporting of infections (baseline characteristics of the NMN and retrospective anti-CD38 cohorts are summarized in Supplementary Table 5). To provide biological context for the observed infection patterns, we examined humoral immune parameters in both cohorts. The low rate and mild course of infection in NMN-treated patients is consistent with preserved humoral immunity, as B cell subset composition, plasmablast cell frequency and circulating immunoglobulin levels remained unchanged throughout the treatment course (Fig. 3i,j, Extended Data Fig. 6m and Supplementary Table 6). By contrast, anti-CD38 mAb therapy led to marked reductions in serum immunoglobulin levels (Extended Data Fig. 6n), consistent with a heightened susceptibility to infections. Taken together, these data suggest that NMN has a favorable safety profile in ITP without compromising humoral immunity.

To exclude a direct effect of NMN on platelet activation and aggregation, we assessed platelet function under NMN exposure in both human and mouse settings. NMN did not measurably alter platelet activation markers or aggregation responses in both healthy controls and WT mice (Supplementary Fig. 7).

We next explored whether NMN treatment modulated systemic inflammatory mediators and whether baseline immune features might relate to clinical response. Plasma cytokine levels showed no significant change from baseline to posttreatment (Supplementary Fig. 8), which may be related to the limited sensitivity of peripheral blood measurements to capture immunopathological changes at key tissue sites of platelet clearance (for example, the spleen). In exploratory analyses, responders exhibited higher baseline CD86 expression on $CD14^+$ monocytes compared to non-responders (Supplementary Fig. 9), suggesting that a heightened inflammatory monocyte state at study entry may be associated with NMN responsiveness. These observations are hypothesis generating and require validation in larger, controlled cohorts.

Discussion

This study supports an immune-metabolic framework in which CD38-mediated NAD^+ depletion is linked to proinflammatory macrophage polarization and accelerates platelet clearance in ITP. By combining genetic and pharmacologic perturbations with metabolic interventions across mouse models and human systems, the CD38–NAD^+ axis was identified as a potential point of therapeutic intervention for antibody-driven cytopenia. Moreover, this study provides the early-phase clinical evidence that low-dose oral NAD^+ precursor supplementation was associated with platelet improvement in a subset of patients, with balanced macrophage activity and preservation of key humoral immune readouts.

Owing to their ability to effectively eliminate both short-lived and long-lived plasma cells, anti-CD38 mAbs have shown promise in refractory autoimmune diseases by reducing autoantibody production[7–14]. In ITP, our previous work and the current analyses extend these observations by highlighting the rapid kinetics of platelet recovery after anti-CD38 treatment, which argues that effector-phase mechanisms

beyond gradual plasma cell depletion are likely to contribute[13,14]. Notably, retreatment with anti-CD38 mAb was followed by similarly rapid platelet recovery and no new safety signals, providing a descriptive indication that readministration can be followed by renewed clinical response in relapsed cases. The similar kinetics observed upon retreatment in relapsed cases further suggests that readministration can be followed by renewed responses in some patients, although these clinical observations are descriptive and will require prospective confirmation.

To investigate the cellular mechanisms underlying this rapid therapeutic effect, we first employed *Cd38*KO passive ITP models and immune cell-specific depletion approaches, which identified macrophages as the principal downstream effector of CD38 in antibody-mediated platelet destruction. CD38 has been extensively studied in the context of infection and cancer. It is highly expressed on proinflammatory (M1) macrophages and further upregulated under inflammatory conditions, where it facilitates macrophage infiltration and proinflammatory cytokine production[46–49]. However, its role in autoimmune dysregulation, particularly its contribution to macrophage-mediated platelet destruction in ITP, remains poorly characterized. In the present study, mechanistic analyses in mouse models and patient samples support a framework in which CD38-mediated NAD^+ depletion is associated with proinflammatory M1 macrophage polarization and Fcγ receptor-dependent platelet clearance in ITP. Accordingly, restoration of NAD^+ levels through NMN supplementation or CD38 inhibition shifted macrophage polarization and ameliorated thrombocytopenia in ITP mice. These results highlight the CD38–NAD^+ axis as an immunometabolic link between macrophage polarization and autoimmune pathology. These findings suggest that the therapeutic effects of anti-CD38 mAb in autoimmunity may reflect complementary mechanisms, including plasma cell depletion[7,8] and macrophage reprogramming. Nevertheless, we cannot exclude the possibility that Fc-opsonized $CD38^+$ plasma cells may transiently divert splenic macrophage phagocytic capacity, conceptually analogous to the proposed 'decoy' mechanism of anti-D immunoglobulin, thereby contributing to the early platelet rise[50]. Although such an occupancy effect could contribute in principle, it may not fully account for the overall response kinetics. Similar Fc opsonization-based 'occupancy' effects would also be expected for other B-cell-targeting antibodies, such as anti-CD20 mAb, yet early platelet rises after anti-CD20 mAb are reported in only a minority of patients, and the typical time to response is substantially longer[51,52]; by contrast, anti-CD38 mAb therapy in our cohorts was characterized by a broadly rapid and consistent platelet recovery in most patients, arguing for additional plasma cell-independent effector-phase mechanisms.

As an autoimmune disease, ITP is primarily driven by aberrant humoral immune responses, in which autoantibody-coated platelets are cleared by the mononuclear phagocyte system through Fcγ receptor-mediated opsonophagocytosis. Across our preclinical models and patient analyses, NMN administration was not accompanied by major changes in B cell subsets, plasma cell frequencies or circulating immunoglobulin levels, and it did not measurably blunt antigen-specific humoral responses in an OVA immunization model, suggesting that NMN exerts limited effects on dysregulated humoral immunity in ITP. Instead, NMN was associated with reduced proinflammatory macrophage polarization, lower FcγRI expression and diminished phagocytic activity, providing a plausible link to attenuated platelet destruction.

In addition to humoral immune abnormalities, T cell dysregulation also contributes to the pathogenesis of ITP. NAD^+ plays a dual role in T cell regulation. On the one hand, NAD^+ is a key metabolic determinant of T cell activation and clonal expansion[53]. On the other hand, NAD^+/SIRT1 signaling influences the expression of lineage-defining transcription factors such as FoxP3 and RORγt, thereby regulating the balance between T regulatory (T_{reg}) cells and T helper 17 (T_H17) cells[54]. Previous studies reported reduced NAD^+ levels in $CD4^+$ T cells from patients with ITP, and supplementation with nicotinamide has been shown to promote T_{reg} cell differentiation; however, such effects were not observed after NMN treatment, which may reflect differences in their engagement of the NAD^+–SIRT1 axis[55]. Taken together, although NMN-mediated elevation of NAD^+ may influence multiple immune cell types, integration of previous literature with our experimental findings suggests that NMN primarily exerts its therapeutic effects in ITP by targeting the Fcγ receptor-dependent platelet clearance phase through immune-metabolic reprogramming.

The emerging field of 'precision immunometabolism' envisions selectively reprogramming cellular metabolism to modulate immune effector function without inducing broad immunosuppression. Although preclinical studies in autoimmune disease models have demonstrated the therapeutic potential of metabolic interventions, clinical evidence remains limited. To bridge this translational gap, we initiated an early-phase, single-arm clinical trial of oral NMN therapy in ITP. This phase 1/2 trial was exploratory in nature, with the primary objective of establishing safety and mechanistic feasibility of a single-metabolite immunometabolic intervention rather than definitive efficacy. The results demonstrated that NMN supplementation safely and effectively induced a rapid and sustained platelet response in most patients. Notably, the modest platelet response may be attributed to the conservative dosing strategy adopted for safety, corresponding to approximately one-third of the mouse therapeutic dose. Notably, too, dose escalation and higher-dose regimens were not evaluated in this study, consistent with the prespecified safety-focused protocol design. Nevertheless, this trial provided the early clinical evidence that targeted metabolic repletion with a single metabolite may rapidly reverse immune-mediated pathology in patients with autoimmune disease.

Conventional immunosuppressants, including corticosteroids, can increase infection risk through broad immune suppression. B-cell-targeted therapies, such as rituximab, daratumumab, bispecific antibodies and chimeric antigen receptor (CAR) T cells, have also been associated with increased risk of infection due to their impairment of humoral immunity[4,15,16]. These limitations underscore the need for safer alternatives that preserve humoral immunity during long-term treatment. In our study, infections were infrequent and mild in the NMN-treated cohort (8%, all grade 1), whereas a higher proportion of infections was observed in the retrospective anti-CD38 mAb cohort (42.9%, any grade); however, these cross-cohort proportions should be interpreted descriptively rather than as a head-to-head comparison, given differences in baseline characteristics and infection ascertainment/reporting. Instead, the safety concept supported by our data is that NMN administration was not accompanied by major changes in humoral immune parameters: NMN treatment did not alter B cell subset composition or plasma cell frequency, reduce circulating immunoglobulin levels or impair antigen-specific humoral responses in an OVA immunization model. By contrast, anti-CD38 mAb therapy depletes $CD38^+$ plasma cells and was associated with reduced serum immunoglobulin levels, consistent with a mechanism that can increase susceptibility to infections. Together, these findings support NMN as a non-depleting immunometabolic strategy that attenuates Fcγ receptor-dependent effector functions while preserving key humoral immune readouts, thereby potentially decoupling therapeutic benefit from broad immunosuppressive burden. This strategy may be applicable not only to ITP but also to other autoantibody-mediated disorders, such as systemic lupus erythematosus and rheumatoid arthritis[30,56,57].

Despite these encouraging outcomes, several critical questions remain. The optimal dosing regimen, durability of clinical benefit and potential long-term immunometabolic consequences of NMN therapy under chronic inflammation remain undefined. Despite clinical platelet improvement in 52% of patients (including partial and suboptimal responses), none achieved complete remission in this

early-phase study. The limited sample size and relatively higher baseline platelet counts of enrolled patients, together with the ethical and safety considerations that precluded enrollment of the most refractory, high-bleeding-risk patients with severe thrombocytopenia, may constrain the generalizability of our findings to more difficult-to-treat populations. Accordingly, larger cohorts and randomized controlled trials, including patients with lower baseline platelet counts and multiple prior treatment failures, are needed to validate efficacy and define durability and long-term safety. In parallel, intervention optimization will be required, including formal dose-finding designs and consideration of combination or sequential regimens (for example, with TPO-RAs or standard-of-care therapies), to enhance efficacy and define durable benefit in more refractory disease. In addition, inter-individual variability in baseline NAD^+ levels, age-associated metabolic decline and comorbid diseases may further influence therapeutic efficacy, highlighting the need for biomarker-guided patient stratification in future precision trials. Bleeding severity was assessed using the WHO Bleeding Scale, which is suboptimal compared to ITP-specific bleeding assessment tools; future prospective studies should incorporate tools such as the Immune Thrombocytopenia Bleeding Scale (IBLS) and the Immune Thrombocytopenia Bleeding Assessment Tool (ITP-BAT).

By integrating mechanistic insight with clinical translation, this study supports the CD38–NAD^+ axis as a candidate metabolic checkpoint in antibody-mediated autoimmunity. In our preclinical and clinical assessments, oral NAD^+ precursor supplementation was associated with attenuation of innate effector programs linked to Fcγ receptor-dependent platelet clearance, whereas key humoral immune readouts were largely preserved. This non-depleting, metabolism-guided approach targets effector-phase inflammatory circuitry rather than broadly suppressing immune function. More broadly, these findings add to growing evidence that immunometabolic reprogramming may provide a precision strategy for reestablishing immune balance in chronic autoimmune disease.

Online content

Any methods, additional references, Nature Portfolio reporting summaries, source data, extended data, supplementary information, acknowledgements, peer review information; details of author contributions and competing interests; and statements of data and code availability are available at https://doi.org/10.1038/s41591-026-04366-x.

References

1. Gatto, M., Zen, M., Cruciani, C., Iaccarino, L. & Doria, A. Navigating the landscape of SLE treatment: an expert viewpoint on the rationality and limitations of early biologic intervention. *Autoimmun. Rev.* **23**, 103612 (2024).
2. Gumkowska-Sroka, O., Kotyla, K., Mojs, E., Palka, K. & Kotyla, P. Novel therapeutic strategies in the treatment of systemic sclerosis. *Pharmaceuticals* **16**, 1066 (2023).
3. Cooper, N. & Ghanima, W. Immune thrombocytopenia. *N. Engl. J. Med.* **381**, 945–955 (2019).
4. Stockfelt, M., Teng, Y. K. O. & Vital, E. M. Opportunities and limitations of B cell depletion approaches in SLE. *Nat. Rev. Rheumatol.* **21**, 111–126 (2025).
5. van Dam, L. S. et al. Highly sensitive flow cytometric detection of residual B-cells after rituximab in anti-neutrophil cytoplasmic antibodies-associated vasculitis patients. *Front. Immunol.* **11**, 566732 (2020).
6. Mahevas, M. et al. Emergence of long-lived autoreactive plasma cells in the spleen of primary warm auto-immune hemolytic anemia patients treated with rituximab. *J Autoimmun.* **62**, 22–30 (2015).
7. Canales-Herrerias, P. et al. High-affinity autoreactive plasma cells disseminate through multiple organs in patients with immune thrombocytopenic purpura. *J. Clin. Invest.* **132**, e153580 (2022).
8. Ostendorf, L. et al. Targeting CD38 with daratumumab in refractory systemic lupus erythematosus. *N. Engl. J. Med.* **383**, 1149–1155 (2020).
9. Jalink, M. et al. Daratumumab monotherapy in refractory warm autoimmune hemolytic anemia and cold agglutinin disease. *Blood Adv.* **8**, 2622–2634 (2024).
10. Strussmann, T. et al. Long-term complete remission of refractory severe idiopathic immune thrombocytopenia (ITP) treated with daratumumab. *Ann. Hematol.* **102**, 245–247 (2023).
11. Vernava, I. & Schmitt, C. A. Daratumumab as a novel treatment option in refractory ITP. *Blood Cells Mol. Dis.* **99**, 102724 (2023).
12. Giammarco, S. et al. The role of daratumumab in complications post-allogeneic hematopoietic stem cell transplantation: a single-center prospective study on PRCA and AIHA. *Bone Marrow Transplant.* **60**, 305–309 (2025).
13. Chen, Y. et al. A novel anti-CD38 monoclonal antibody for treating immune thrombocytopenia. *N. Engl. J. Med.* **390**, 2178–2190 (2024).
14. Sun, T., Chen, Y. & Zhang, L. Daratumumab in relapsed or refractory pediatric immune thrombocytopenia. *N. Engl. J. Med.* **392**, 2069–2071 (2025).
15. Holzer, M. T. et al. Daratumumab for autoimmune diseases: a systematic review. *RMD Open* **9**, e003604 (2023).
16. Otani, I. M. et al. Practical guidance for the diagnosis and management of secondary hypogammaglobulinemia: a Work Group Report of the AAAAI Primary Immunodeficiency and Altered Immune Response Committees. *J. Allergy Clin. Immunol.* **149**, 1525–1560 (2022).
17. Hooftman, A. et al. Macrophage fumarate hydratase restrains mtRNA-mediated interferon production. *Nature* **615**, 490–498 (2023).
18. Ziegler, J. F. et al. Leptin induces TNFα-dependent inflammation in acquired generalized lipodystrophy and combined Crohn's disease. *Nat. Commun.* **10**, 5629 (2019).
19. Zheng, X., Tsou, P. S. & Sawalha, A. H. Increased expression of EZH2 is mediated by higher glycolysis and mTORC1 activation in lupus $CD4^+$ T cells. *Immunometabolism* **2**, e200013 (2020).
20. Wei, J. et al. Elevated fatty acid β-oxidation by leptin contributes to the proinflammatory characteristics of fibroblast-like synoviocytes from RA patients via LKB1-AMPK pathway. *Cell Death Dis.* **14**, 97 (2023).
21. Legroux, T. M. et al. Immunomodulation by glucocorticoid-induced leucine zipper in macrophages: enhanced phagocytosis, protection from pyroptosis, and altered mitochondrial function. *Front. Immunol.* **15**, 1396827 (2024).
22. Li, X. et al. Excess glucocorticoids inhibit murine bone turnover via modulating the immunometabolism of the skeletal microenvironment. *J. Clin. Invest.* **134**, e166795 (2024).
23. Gan, P. X. L., Liao, W., Lim, H. F. & Wong, W. S. F. Dexamethasone protects against *Aspergillus fumigatus*-induced severe asthma via modulating pulmonary immunometabolism. *Pharmacol. Res.* **196**, 106929 (2023).
24. Auger, J. P. et al. Metabolic rewiring promotes anti-inflammatory effects of glucocorticoids. *Nature* **629**, 184–192 (2024).
25. Jenkins, B. J. et al. Canagliflozin impairs T cell effector function via metabolic suppression in autoimmunity. *Cell Metab.* **35**, 1132–1146 (2023).
26. Montano, E. N. et al. α-Ketoglutarate–dependent KDM6 histone demethylases and interferon-stimulated gene expression in lupus. *Arthritis Rheumatol.* **76**, 396–410 (2024).
27. Pan, W., Tsokos, M. G., Scherlinger, M., Li, W. & Tsokos, G. C. The PP2A regulatory subunit PPP2R2A controls NAD^+ biosynthesis to regulate T cell subset differentiation in systemic autoimmunity. *Cell Rep.* **43**, 114379 (2024).

28. Masuyama, S. et al. Enhanced fatty acid oxidation by selective activation of PPARα alleviates autoimmunity through metabolic transformation in T-cells. *Clin. Immunol.* **268**, 110357 (2024).
29. Angiari, S. et al. Coenzyme A fueling with pantethine limits autoreactive T cell pathogenicity in experimental neuroinflammation. *J. Neuroinflammation* **21**, 287 (2024).
30. Jia, N. et al. Metabolic reprogramming of proinflammatory macrophages by target delivered roburic acid effectively ameliorates rheumatoid arthritis symptoms. *Signal Transduct. Target. Ther.* **8**, 280 (2023).
31. Meyer, T. et al. NAD^+ metabolism drives astrocyte proinflammatory reprogramming in central nervous system autoimmunity. *Proc. Natl Acad. Sci. USA* **119**, e2211310119 (2022).
32. Gil Alabarse, P., Chen, L. Y., Oliveira, P., Qin, H. & Liu-Bryan, R. Targeting CD38 to suppress osteoarthritis development and associated pain after joint injury in mice. *Arthritis Rheumatol.* **75**, 364–374 (2023).
33. Covarrubias, A. J., Perrone, R., Grozio, A. & Verdin, E. NAD^+ metabolism and its roles in cellular processes during ageing. *Nat. Rev. Mol. Cell Biol.* **22**, 119–141 (2021).
34. Minhas, P. S. et al. Macrophage de novo NAD^+ synthesis specifies immune function in aging and inflammation. *Nat. Immunol.* **20**, 50–63 (2019).
35. Feng, Q. et al. High-dose dexamethasone or all-trans-retinoic acid restores the balance of macrophages towards M2 in immune thrombocytopenia. *J. Thromb. Haemost.* **15**, 1845–1858 (2017).
36. Liang, Z. et al. Mesenchymal stromal cells regulate M1/M2 macrophage polarization in mice with immune thrombocytopenia. *Stem Cells Dev.* **32**, 703–714 (2023).
37. Zhao, H. Y. et al. M2 macrophages, but not M1 macrophages, support megakaryopoiesis by upregulating PI3K-AKT pathway activity. *Signal Transduct. Target. Ther.* **6**, 234 (2021).
38. Kasperczyk, H. et al. Betulinic acid as new activator of NF-κB: molecular mechanisms and implications for cancer therapy. *Oncogene* **24**, 6945–6956 (2005).
39. Tien, T. Y. et al. Reduction of connexin 43 attenuates angiogenic effects of human smooth muscle progenitor cells via inactivation of Akt and NF-κB pathway. *Arterioscler. Thromb. Vasc. Biol.* **41**, 915–930 (2021).
40. Hoffmann, A., Cheng, G. & Baltimore, D. NF-κB: master regulator of cellular responses in health and disease. *Immun. Inflamm.* **1**, 2 (2025).
41. Liu, J., Chen, Y. & O' Neill, L. Phospholipid metabolism in innate immunity and inflammation: from basic to clinic. *Immun. Inflamm.* **1**, 6 (2025).
42. Irie, J. et al. Effect of oral administration of nicotinamide mononucleotide on clinical parameters and nicotinamide metabolite levels in healthy Japanese men. *Endocr. J.* **67**, 153–160 (2020).
43. Mitchell, S. J. et al. Nicotinamide improves aspects of healthspan, but not lifespan, in mice. *Cell Metab.* **27**, 667–676 (2018).
44. Yoshino, M. et al. Nicotinamide mononucleotide increases muscle insulin sensitivity in prediabetic women. *Science* **372**, 1224–1229 (2021).
45. Malique, A. et al. NAD^+ precursors and bile acid sequestration treat preclinical refractory environmental enteric dysfunction. *Sci. Transl. Med.* **16**, eabq4145 (2024).
46. Jablonski, K. A. et al. Novel markers to delineate murine M1 and M2 macrophages. *PLoS ONE* **10**, e0145342 (2015).
47. Wen, S., Arakawa, H. & Tamai, I. CD38 activation by monosodium urate crystals contributes to inflammatory responses in human and murine macrophages. *Biochem. Biophys. Res. Commun.* **581**, 6–11 (2021).
48. Lory, W. et al. CD38 inhibitor 78c attenuates pro-inflammatory cytokine expression and osteoclastogenesis in macrophages. *Cells* **13**, 1971 (2024).
49. Ma, Y. et al. Deletion of CD38 mitigates the severity of NEC in experimental settings by modulating macrophage-mediated inflammation. *Redox Biol.* **77**, 103336 (2024).
50. Bussel, J. B. et al. Intravenous anti-D treatment of immune thrombocytopenic purpura: analysis of efficacy, toxicity, and mechanism of effect. *Blood* **77**, 1884–1893 (1991).
51. Khellaf, M. et al. Safety and efficacy of rituximab in adult immune thrombocytopenia: results from a prospective registry including 248 patients. *Blood* **124**, 3228–3236 (2014).
52. Bennett, C. M. et al. Prospective phase 1/2 study of rituximab in childhood and adolescent chronic immune thrombocytopenic purpura. *Blood* **107**, 2639–2642 (2006).
53. Mann, R., Stavrou, V. & Dimeloe, S. NAD + metabolism AND function in innate AND adaptive immune cells. *J. Inflamm.* **22**, 30 (2025).
54. Navarro, M. N., Gómez de Las Heras, M. M. & Mittelbrunn, M. Nicotinamide adenine dinucleotide metabolism in the immune response, autoimmunity and inflammageing. *Br. J. Pharmacol.* **179**, 1839–1856 (2022).
55. Li, J. et al. Nicotinamide enhances Treg differentiation by promoting Foxp3 acetylation in immune thrombocytopenia. *Br. J. Haematol.* **205**, 2432–2441 (2024).
56. Jing, C. et al. Macrophage metabolic reprogramming presents a therapeutic target in lupus nephritis. *Proc. Natl Acad. Sci. USA* **117**, 15160–15171 (2020).
57. Cuda, C. M., Pope, R. M. & Perlman, H. The inflammatory role of phagocyte apoptotic pathways in rheumatic diseases. *Nat. Rev. Rheumatol.* **12**, 543–558 (2016).

Huiyuan Li[1,2,3], Yuan Xu[1,2,3], Yunfei Chen[1,2,3], Lulu Ji[1,2,3], Yanmei Xu[1,2,3], Wenting Zheng[1,2], Ting Sun[1,2], Rongfeng Fu[1,2], Xiaolei Pei[1,2], Xiaofan Liu[1,2], Feng Xue[1,2], Wei Liu[1,2], Wentian Wang[1,2], Ying Chi[1,2], Renchi Yang[1,2], Jun Wei[1,2] ✉ & Lei Zhang[1,2] ✉

[1]State Key Laboratory of Experimental Hematology, National Clinical Research Center for Blood Diseases, Haihe Laboratory of Cell Ecosystem, Tianjin Key Laboratory of Gene Therapy for Blood Diseases, Institute of Hematology & Blood Diseases Hospital, Chinese Academy of Medical Sciences & Peking Union Medical College, Tianjin, China. [2]Tianjin Institutes of Health Science, Tianjin, China. [3]These authors contributed equally: Huiyuan Li, Yuan Xu, Yunfei Chen, Lulu Ji, Yanmei Xu. ✉e-mail: weijun@ihcams.ac.cn; zhanglei1@ihcams.ac.cn

Methods

Patients

This study was carried out in compliance with the principles outlined in the Declaration of Helsinki. All participants provided written informed consent after a comprehensive explanation of study objectives and procedures. Participants received no financial compensation for participation in this study. The study protocol was approved by the Ethics Committee of the Institute of Hematology and Blood Diseases Hospital. Eligible patients were diagnosed with primary ITP based on established international consensus guidelines[58]. Patients with secondary ITP or those who were pregnant were excluded from the study.

Study design. This work comprised four complementary human study components in adults with primary ITP and controls: (1) a retrospective, single-center, anti-CD38 mAb treatment cohort; (2) a retrospective anti-CD38 mAb retreatment cohort in relapsed patients; (3) a prospective, phase 1/2, single-arm, open-label clinical trial of oral NMN; and (4) translational mechanistic studies using spleen tissue, peripheral blood and MDMs from patients with ITP and non-ITP controls.

Participant sex (male/female) was recorded based on medical records at enrollment or at the time of clinical sampling. Sex was considered in the study design and recruitment to support balanced representation across study groups where applicable; sex-stratified analyses were not prespecified because the study was not powered for sex-based comparisons.

Retrospective anti-CD38 mAb treatment cohort. To characterize the temporal dynamics of platelet response to CD38 blockade, a retrospective, single-center study was conducted involving 21 patients. Patients were eligible if they were adults (≥18 years of age) who received at least eight weekly intravenous infusions of anti-CD38 mAb (16 mg kg^{-1}) between September and December 2024, met the diagnostic criteria for primary ITP, had platelet count $<30 \times 10^9$ per liter and had persistent or chronic ITP. All patients were followed for at least 24 weeks after the first infusion. Patients with secondary ITP or pregnancy were excluded. Baseline demographic and clinical characteristics are summarized in Extended Data Table 3 and Supplementary Table 5.

Retrospective anti-CD38 mAb retreatment cohort in relapsed patients. To assess the efficacy of readministration in the setting of relapse, a separate retrospective cohort was assembled comprising three adult patients with primary ITP who relapsed after an initial response and subsequently received four additional weekly intravenous infusions of anti-CD38 mAb (16 mg kg^{-1}). The retreatment cohort was analyzed separately owing to differences in follow-up procedures and was not part of the initial 21-patient cohort. Baseline demographic and clinical characteristics are summarized in Extended Data Table 3.

Prospective NMN clinical trial. *Design and oversight*. A phase 1/2, investigator-initiated, single-arm, open-label clinical trial was conducted to evaluate the safety and efficacy of oral NMN in adults with ITP (ClinicalTrials.gov identifier: NCT06776510). The trial comprised a 4-week screening phase, a 2-week treatment phase and a 6-week follow-up period. NMN was administered orally at a dose of 450 mg twice daily for 2 weeks. The study was conducted in accordance with the Declaration of Helsinki and Good Clinical Practice guidelines and was approved by the institutional ethics committee; all participants provided written informed consent before enrollment. As an investigator-initiated, low-risk, exploratory study with a small sample size, no data and safety monitoring board was convened; safety was overseen by the institutional ethics committee and monitored according to the prespecified protocol. No protocol amendments affecting eligibility criteria, endpoints or dosing were introduced. The protocol and the statistical analysis plan are available in Supplementary Information.

Concomitant treatment with a single maintenance ITP therapy was permitted. Eligible concomitant medications included corticosteroids at ≤0.5 mg kg^{-1} prednisone-equivalent or TPO-RAs. At enrollment, each patient could receive no more than one such concomitant agent, which had to be on a stable dose for at least 4 weeks prior to the first NMN dose. Dose escalation of concomitant therapies and initiation of new platelet-elevating treatments (including high-dose corticosteroids, IVIG, platelet transfusion or additional TPO-RAs) were not permitted during the study, except as protocol-defined emergency rescue therapy, in which case efficacy endpoints were censored and patients were considered non-responders for the primary efficacy analysis.

Inclusion and exclusion criteria. Participants were eligible if they met all of the following inclusion criteria: (1) age ≥18 years, male or female; (2) diagnosis of primary ITP according to established criteria with a disease duration ≥3 months; (3) failure to achieve a response or relapse after at least one corticosteroid therapy and either failure to achieve a response or relapse after previous second-line treatments, such as TPO/TPO-RAs, or unable to afford the cost of the treatment; (4) platelet count $<30 \times 10^9$ per liter within 2 days prior to enrollment, confirmed on at least two consecutive measurements spaced by a minimum of 1 day, obtained during the screening visit and/or immediately before the first NMN administration; (5) ECOG performance status ≤2; (6) on a stable dose of no more than one maintenance ITP therapy (corticosteroids ≤0.5 mg kg^{-1} prednisone-equivalent or a TPO-RA) for at least 4 weeks prior to the first dose of NMN; (7) for females of childbearing potential, a negative pregnancy test at screening and, for all females of childbearing potential and all males, agreement to use highly effective contraception during the study and for at least 4 months (women) or 6 months (men) after discontinuing NMN; and (8) ability to understand the study requirements and provision of signed and dated informed consent.

Participants were excluded if any of the following criteria applied: (1) known hypersensitivity to NMN, NAD or any formulation excipients or documented failure to respond to prior anti-CD38 mAb therapy; (2) secondary or hereditary thrombocytopenia, including, but not limited to, autoimmune hemolytic anemia, leukemia, lymphoma, multiple myeloma, aplastic anemia, myelodysplastic syndrome, Evans syndrome, common variable immunodeficiency, systemic lupus erythematosus, cirrhosis, antiphospholipid antibody syndrome, pseudothrombocytopenia and drug-induced thrombocytopenia (for example, quinine, heparin, antimicrobial drugs and anticonvulsants); (3) history of thrombosis or embolism within 12 months prior to the first dose or the presence of extensive and severe bleeding, such as hemoptysis, upper gastrointestinal bleeding, intracranial hemorrhage, sepsis or other unstable major bleeding; (4) participation in another investigational drug trial (including vaccines) or exposure to other investigational drugs within 4 weeks or five half-lives (whichever was longer) before the first dose; (5) use of anticoagulants or drugs with antiplatelet effects (for example, aspirin) within 2 weeks prior to the first dose; (6) receipt of emergency ITP treatment (for example, high-dose methylprednisolone, platelet transfusion, IVIG or TPO-RA treatment) within 2 weeks prior to enrollment; (7) use of azathioprine, danazol, cyclosporine A, tacrolimus or sirolimus within 4 weeks or anti-CD20 mAbs (for example, rituximab), cyclophosphamide or vincristine within 3 months prior to the first dose; (8) splenectomy within 6 months prior to the first dose; (9) receipt of a live attenuated vaccine within 4 weeks prior to treatment or planned receipt of a live attenuated vaccine during the study; (10) history of allogeneic stem cell or solid organ transplantation; (11) any clinically significant disease that, in the investigator's opinion, could pose an unacceptable risk to the patient's safety or confound assessment of safety or efficacy if the condition worsened during the study; (12) malignant tumors within 5 years prior to screening (excluding completely resected carcinoma in situ of the cervix and non-metastatic squamous cell or basal cell carcinoma of the skin);

(13) clinically significant laboratory abnormalities at screening, including alanine aminotransferase or aspartate aminotransferase ≥upper limit of normal (ULN), total bilirubin ≥1.2× ULN or creatinine or blood urea nitrogen ≥ULN; (14) positive screening for HIV or syphilis antibodies; (15) positive hepatitis B surface antigen or positive hepatitis B core antibodies with detectable hepatitis B virus DNA by polymerase chain reaction (PCR) or positive hepatitis C virus antibodies; (16) pregnancy or breastfeeding or plans to become pregnant or breastfeed during the study; (17) psychiatric or cognitive impairment precluding informed consent or compliance with the protocol; (18) unresolved toxicity from prior treatments at the time of screening; or (19) any other condition deemed unsuitable for participation by the investigator.

Endpoints. The prespecified primary endpoints included (1) safety and tolerability of NMN, assessed by the incidence and severity of treatment-emergent adverse events and SAEs and by routine laboratory tests, with severity graded according to NCI-CTCAE version 5.0; and (2) efficacy, defined as the proportion of patients achieving a platelet count ≥50×10^9 per liter within 2 weeks of treatment initiation, confirmed by two consecutive measurements at least 1 day apart, in the absence of rescue therapy and without any dose increment of TPO-RAs or corticosteroids during the study period.

Secondary endpoints included (1) the proportion of patients with a platelet count ≥50×10^9 per liter at weeks 1, 2, 3, 4, 6 and 8, under the same no-rescue/no-dose-escalation conditions; (2) time from treatment initiation to platelet counts ≥30×10^9 per liter (at least a two-fold increase from baseline) and ≥50×10^9 per liter, without receipt of any platelet-elevating therapy or dose increment of TPO-RAs and/or corticosteroids; (3) platelet count values at each prespecified visit (day 0 and weeks 1–8); (4) the proportion of patients who received emergency rescue treatment within 2 weeks and during the entire study period; (5) cumulative weeks with platelet counts ≥30×10^9 per liter (at least two-fold from baseline) and ≥50×10^9 per liter, without receipt of any platelet-elevating therapy or dose increment of TPO-RAs and/or corticosteroids; (6) the change in WHO bleeding score from baseline to 2 weeks after treatment, using the WHO Bleeding Scale (grade 0, no bleeding; grade 1, petechiae; grade 2, mild blood loss; grade 3, gross blood loss; grade 4, debilitating blood loss); (7) the proportion of patients achieving platelet count ≥50×10^9 per liter at least once within the first 4 weeks, without rescue therapy or dose escalation of TPO-RAs or corticosteroids; (8) the proportion of patients whose platelet count reached ≥30×10^9 per liter and at least two-fold from baseline within 4 weeks (two consecutive measurements at least 7 days apart), without rescue therapy or dose escalation of TPO-RAs or corticosteroids; and (9) the proportion of patients with a suboptimal response at each visit, defined as a platelet count ≥30×10^9 per liter with a ≥1.5-fold but <2-fold increase from baseline and no bleeding, confirmed by at least two platelet count measurements taken at least 7 days apart.

Response definitions. To more comprehensively assess treatment efficacy, we predefined modified response categories for ITP. Complete response was defined as a posttreatment platelet count ≥100×10^9 per liter without bleeding, confirmed by at least two assessments performed at least 7 days apart. Partial response was defined as platelet counts ≥30×10^9 per liter and <100×10^9 per liter, with a ≥2-fold increase from the baseline platelet count and no bleeding, confirmed by at least two assessments at least 7 days apart. Suboptimal response was defined as a platelet count ≥30×10^9 per liter with a ≥1.5-fold but <2-fold increase from baseline and no bleeding, confirmed by at least two platelet count measurements taken at least 7 days apart. No response was defined as failure to meet the criteria for complete response, partial response or suboptimal response. Relapse was defined as any of the following after an initial response: a platelet count <30×10^9 per liter or <1.5-fold increase from baseline or the occurrence of clinical bleeding. Complete response, partial response and suboptimal response required confirmation by at least two platelet measurements obtained at least 7 days apart; no response and relapse required confirmation by at least two assessments performed at least 1 day apart.

Sample size estimation

For adult patients with primary ITP who had failed to achieve or maintain a response after corticosteroid therapy and had either failed prior second-line treatments or lacked financial access to such therapies, we assumed that the proportion of patients achieving a platelet count ≥50×10^9 per liter within 8 weeks after treatment would be 55%, with a null (target) value of 20%. With a two-sided type I error of 0.05, a planned sample size of 16 patients would provide 85.6% power to test the hypothesis that the primary efficacy endpoint exceeds the target value, as calculated using PASS software. Allowing for an anticipated dropout rate of approximately 20%, the planned enrollment was at least 20 patients; ultimately, 25 patients were enrolled to ensure an adequate number of evaluable participants.

Efficacy analyses were performed in the intention-to-treat population, defined as all enrolled patients. Safety analyses were performed in the safety population, defined as all patients who received at least one dose of NMN. A total of 25 patients were enrolled; detailed baseline clinical characteristics and concomitant medication use are reported in Table 1 and Extended Data Table 4, respectively.

Translational studies in spleen tissue, peripheral blood and MDMs. For mechanistic experiments, spleen tissue and peripheral blood samples were obtained from patients and controls. Spleen tissues were collected from 21 patients with ITP who underwent therapeutic splenectomy and from seven trauma patients without hematologic or autoimmune disease serving as controls. Immunofluorescence staining was performed on 18 samples, and scRNA-seq was conducted on samples from eight patients with ITP and four trauma controls. In addition, to characterize treatment-associated immune changes in the mechanistic cohort, peripheral blood samples were collected from nine patients treated with anti-CD38 mAb (five sustained responders and four relapsed cases) at baseline (day 0) and posttreatment (day 56) for scRNA-seq. Plasma samples from 14 sustained responders treated with anti-CD38 mAb were collected at baseline (day 0) and day 8 for Olink proteomic profiling. For in vitro functional assays, MDMs were generated from 27 patients with ITP and from 42 age-matched and sex-matched healthy controls. These MDMs were used in NAD^+ modulation experiments involving NMN and anti-CD38 mAb treatments. In addition, platelets from an independent cohort of 18 healthy controls were used to assess the effects of NMN on platelet activation and function. Detailed clinical information for all enrolled patients with ITP is provided in Extended Data Table 3.

Mice

BALB/c and C57BL/6J (CD45.2) mice were purchased from Beijing HFK Bioscience Co., Ltd. CD45.1 congenic mice (B6.SJL-Ptprca Pepcb/BoyJ; stock no. 002014) were obtained from The Jackson Laboratory. *Cd38* knockout (CD38KO, $CD38^{-/-}$) mice (C57BL/6Smoc-*Cd38*^{em2Smoc}, CD45.2; stock no. NM-KO-226125) on a C57BL/6J background were purchased from Shanghai Model Organisms Center. Lyz2-iCre mice (C57BL/6JGpt-*Lyz2*$^{em1Cin(iCre)}$/Gpt, stock no. T003822) and *Cd38*-flox mice (C57BL/6JGpt-*Cd38*^{em1Cflox}/Gpt, stock no. T009317) were purchased from GemPharmatech and crossed to generate *Cd38*$^{fl/fl}$;*Lyz2*$^{iCre+}$ (myeloid-specific *Cd38* conditional knockout) mice and *Cd38*$^{fl/fl}$;*Lyz2*$^{iCre-}$ littermate controls. Genotyping was performed using genomic DNA extracted from tail biopsies, following the manufacturer's protocol.

Experiments using *Cd38*-deficient models, including *Cd38*KO mice and *Cd38*KO hematopoietic stem cell (HSC) transplantation, were performed on a C57BL/6J background, with age-matched and sex-matched C57BL/6J WT mice (or WT HSC transplantation controls, as applicable). Unless otherwise specified, passive ITP induction, immune cell

depletion and pharmacological intervention studies of NMN or the CD38 inhibitor 78c were performed in BALB/c mice (8–10 weeks old), whereas CD38 KO, bone marrow transplantation and myeloid-specific deletion experiments were performed on a C57BL/6J background using the corresponding strains described above. All experimental comparisons were performed within the same genetic background, and no cross-strain comparisons were made. All animals were housed under standard conditions, with controlled temperature (approximately 25 °C), relative humidity of 40–70% and a 14-hour light/10-hour dark cycle. Mice were randomly assigned to experimental groups and used at 8–10 weeks of age. All animal procedures were performed in accordance with institutional guidelines and approved by the Institutional Animal Care and Use Committee of the Institute of Hematology and Blood Disease Hospital, Chinese Academy of Medical Sciences. Where applicable, we represent pooled results from at least two independent experiments; *n* values indicate the total number of mice across experiments. In each mouse experimental batch, the sex ratio was approximately balanced across treatment groups.

Passive mouse model of ITP

To induce ITP, mice received intraperitoneal injections of anti-mouse CD41 mAb (clone MWReg30; BioLegend, 133902) at an initial dose of 68 μg kg^{-1} body weight, followed by escalating doses, as described previously[59]. Platelet counts were monitored daily using tail vein blood samples (from day 0 to day 6) using an automated hematology analyzer (Mindray).

In vivo immune cell depletion

Selective immune cell populations were depleted by intraperitoneal administration of the following reagents at defined intervals relative to anti-CD41 mAb induction. On days −1 and +2, mice received 500 μg of InVivoMAb anti-mouse CD19 antibody (clone 1D3; Bio X Cell, BE0150) for B cell depletion; 200 μg of InVivoMAb anti-mouse CD4 (clone GK1.5; Bio X Cell, BE0003) or anti-mouse CD8 (clone 2.43; Bio X Cell, BE0061) antibodies for $CD4^+$ and $CD8^+$ T cell depletion, respectively. For macrophage depletion, 200 μl of clodronate-containing liposomes (C-005, clodronateliposomes) was used, with PBS-loaded liposomes as control. Neutrophil depletion was achieved with 100 μg of anti-Ly-6G antibody (clone 1A8; Bio X Cell, BE0075) on day −1, followed by 50 μg on days +1 and +3. Natural killer cells were depleted with 50 μl of anti-Asialo-GM1 polyclonal antibody (clone Poly21460; BioLegend, 146002) administered on days −1 and +2.

Bone marrow transplantation

CD45.1 recipient mice (8–10 weeks old) received lethal irradiation delivered as two split doses of 4 Gy spaced 4 hours apart. Donor bone marrow cells were harvested from the femurs and tibias of age-matched C57BL/6J or *Cd38*KO donor mice. Four hours after the second irradiation, 1×10^6 donor cells suspended in 300 μl of PBS were injected into the tail vein of each recipient mouse.

After transplantation, mice were maintained in sterile cages with access to autoclaved food and water. Broad-spectrum antibiotics were administered via drinking water starting 3 days prior to transplantation and continued for 2 weeks after transplantation. Six weeks after transplantation, peripheral blood chimerism was assessed via flow cytometry on tail vein blood, using $CD45.1^+$ (host) and $CD45.2^+$ (donor) markers. Mice with ≥90% donor-derived leukocytes were included for subsequent passive ITP modeling.

Induction and treatment of BMDMs

Bone marrow cells were isolated by flushing femurs and tibias with sterile PBS, followed by filtration through a 70-μm cell strainer. Red blood cells were lysed using ACK buffer (Gibco, A1049201) to obtain a single-cell suspension. Cells were resuspended in complete Iscove's Modified Dulbecco's Medium (IMDM) supplemented with 10% FBS (Gibco, 10099141C), 1% penicillin–streptomycin and 30 ng ml^{-1} recombinant murine M-CSF (R&D Systems, 416-ML) and seeded at 1×10^6 per well in six-well plates. Cultures were maintained at 37 °C in a humidified 5% CO_2 incubator for 6 days. Media were half-refreshed every 3 days to promote macrophage differentiation.

Macrophage depletion and BMDM adoptive transfer followed by passive ITP induction

WT recipient mice were treated with clodronate liposomes (200 μl per mouse) to deplete tissue macrophages. Twenty-four hours later, ex vivo-generated BMDMs from WT or *Cd38*KO donor mice (3×10^6 cells per mouse) were transferred intravenously via the tail vein. After an additional 24 hours, passive ITP was induced by a single intraperitoneal injection of anti-CD41 antibody (68 μg kg^{-1}). Peripheral blood was collected at baseline (0 hours) and at 2, 4, 8, 12, 24, 48 and 72 hours after anti-CD41 administration, and platelet counts were determined as described above.

Transcriptomic profiling

Differentiated BMDMs were treated with 30 ng ml^{-1} LPS (Sigma-Aldrich, L4391) for 72 hours in the presence or absence of 20 μg ml^{-1} 78c (MedChemExpress, HY-123999) or 200 μg ml^{-1} NMN (Aladdin, 1094-61-7). Adherent cells were collected using Accutase (Gibco, A1110501), lysed using TRIzol reagent (Invitrogen, 15596026) and thoroughly homogenized. Total RNA was extracted according to the manufacturer's instructions. RNA-seq was performed using the Illumina NovaSeq platform and analyzed by LC-Bio Technologies.

Immunofluorescence staining

Spleens were harvested and fixed overnight in 4% paraformaldehyde (PFA), followed by dehydration, paraffin embedding and sectioning into 4-μm-thick slices. Tissue sections were deparaffinized in xylene, rehydrated through a graded ethanol series and subjected to antigen retrieval using EDTA buffer (pH 9.0) in a pressure cooker. After cooling and washing with Tris-buffered saline with Tween 20 (TBST), endogenous peroxidase activity was quenched using 3% hydrogen peroxide (H_2O_2). Sections were blocked with 10% goat serum at 37 °C for 30 minutes and then incubated overnight at 4 °C with primary antibodies. Mouse spleen sections were stained for F4/80 (clone D2S9R; Cell Signaling Technology, 70076, 1:8,000), CD38 (clone EPR21079; Abcam, ab216343, 1:2,000), CD163 (clone EPR19518; Abcam, ab182422) and iNOS (clone RM1017; Abcam, ab283655, 1:1,000) using a multiplex tyramide signal amplification (TSA) workflow. Human spleen sections were stained for CD68 (clone C68/684; Abcam, ab201340, 1:100), CD38 (clone EPR4106; Abcam, ab108403, 1:2,000), CD163 (clone EPR19518; Abcam, ab182422, 1:4,000) and iNOS (clone RM1017; Abcam, ab283655, 1:200), with iNOS and CD68 detected using conventional fluorophore-conjugated secondary antibodies and CD38/CD163 detected using TSA.

Mouse spleen (multiplex TSA). For sequential multiplex detection, sections were incubated with the corresponding primary antibody, followed by HRP-conjugated goat anti-rabbit IgG (Abcam, ab205718) at 37 °C for 45 minutes and TSA according to the manufacturer's instructions using spectrally distinct fluorophore-conjugated tyramides (AAT Bioquest): iNOS, iFluor 488 tyramide (11060); F4/80, Cy3 tyramide (11065); CD38, Cy5 tyramide (11066); and CD163, iFluor 430 tyramide (45096). Sections were extensively washed with TBST between steps, and antigen retrieval was repeated prior to each additional primary antibody staining cycle to enable sequential multiplexing.

Human spleen (mixed TSA and conventional immunofluorescence). For TSA-based targets (CD38 and CD163), sections were processed as above using HRP-conjugated goat anti-rabbit IgG (Abcam, ab205718) and TSA with spectrally distinct tyramides (CD38, iFluor 430 tyramide

(45096) and CD163, Cy5 tyramide (11066)). For conventional immunofluorescence targets, iNOS was detected using Donkey anti-Rabbit IgG (H + L) Highly Cross-Adsorbed Secondary Antibody, Alexa Fluor 488 (Thermo Fisher Scientific, A21206, 1:400), and CD68 was detected using Donkey anti-Mouse IgG (H + L) Highly Cross-Adsorbed Secondary Antibody, Alexa Fluor Plus 555 (Thermo Fisher Scientific, A32773, 1:500). Conventional secondary antibodies were incubated at 37 °C for 45 minutes.

Nuclei were counterstained with DAPI for 5 minutes, and slides were mounted with anti-fade medium. Fluorescent images were acquired using a high-resolution fluorescence microscope (Pannoramic MIDI) using CaseViewer (version 2.4) software with identical acquisition settings across all samples. Fluorescence channels are shown in pseudocolor; for consistency with mouse images, CD163 and CD38 display colors were swapped in the human panels for presentation only (without altering signal intensities). Image processing and quantification were performed using ImageJ version 1.54 software.

In vivo platelet clearance assay

Platelets were isolated from citrate-anticoagulated whole blood using sequential centrifugation and resuspended in modified Tyrode's buffer (Leagene Biotechnology, CZ0064) at a final concentration of 1×10^9 cells per milliliter. Cells were labeled with 5 µM CellTrace Violet (Thermo Fisher Scientific, C34557) for 20 minutes at 37 °C. Excess dye was removed by washing with complete IMDM. Labeled platelets were then opsonized with 5 µg ml^{-1} anti-CD41 antibody (clone MWReg30; BioLegend, 133902) at 37 °C for 20 minutes and washed twice with PBS. A total of 1×10^8 labeled, opsonized platelets in 200 µl of PBS containing 1 mM EDTA were transfused into recipient mice via tail vein injection. Blood samples were collected from the tail vein at baseline (pre-transfusion), 1 minute (designated as 0 hours) and 2 hours post-transfusion into acid–citrate–dextrose (ACD; Beyotime Biotechnology, ST496) anticoagulant (blood:ACD = 7:1, v/v). Circulating labeled platelets were quantified by flow cytometry.

For flow cytometric analysis, platelet-rich plasma (PRP) was obtained by centrifuging whole blood at 200*g* for 10 minutes to remove leukocytes and erythrocytes. The resulting PRP was diluted in PBS and analyzed by a FongCyte flow cytometer (Challenbio), gating on forward scatter and side scatter (FSC/SSC) and CellTrace Violet positivity. The gating strategy is shown in Supplementary Fig. 10. Data were processed using FlowJo version 10 software (TreeStar).

Isolation of spleen single-cell suspensions and PBMCs

Spleens were mechanically dissociated in ice-cold PBS using a sterile tissue grinder, and the resulting cell suspensions were filtered through a 70-µm cell strainer to remove debris. Red blood cells were lysed using ACK buffer to obtain pure splenic single-cell suspensions.

For PBMC isolation, peripheral blood was subjected to density gradient centrifugation using Ficoll-Paque (Haoyang Biotech, LTS1077) according to standard protocols.

Assessment of CD38 deletion efficiency in splenic macrophages by flow cytometry

To assess *Cd38* deletion efficiency in myeloid-specific *Cd38* conditional knockout mice, splenic single-cell suspensions were prepared from $Cd38^{fl/fl}Lyz2^{iCre+}$ and $Cd38^{fl/fl}Lyz2^{iCre-}$ littermate controls. Cell suspensions were adjusted to 2×10^7 cells per milliliter, and 100 µl was used for staining. Samples were incubated with APC-conjugated anti-F4/80 (clone BM8; BioLegend, 123116), PE-Cy7-conjugated anti-CD11b (clone M1/70; BioLegend, 101216) and FITC-conjugated anti-CD38 (clone 90; BioLegend, 102705) for 15 minutes at room temperature in the dark, washed with PBS and fixed with 2% PFA prior to acquisition. All fluorochrome-conjugated antibodies used for flow cytometry in this study were used at 5 µl per test according to the manufacturers' recommendations, unless otherwise specified. All samples were acquired on a FongCyte flow cytometer, and data were analyzed using FlowJo version 10.0. The gating strategy is shown in Supplementary Fig. 10.

scRNA-seq and analysis

Spleen cells and PBMCs were resuspended in 0.01% BSA dissolved in Dulbecco's PBS at a final concentration of 1,000 cells per microliter. Single-cell libraries were prepared using the Chromium Single Cell 5′ Kit (10x Genomics) and sequenced on the Illumina NovaSeq platform, capturing 5,000–10,000 cells per sample. Raw sequencing data were processed using Cell Ranger (version 3.1.0) with alignment to the GRCh38 human reference genome. Downstream analysis was conducted in Seurat version 4.1.1 (ref. 60). Quality control excluded cells with aberrant mitochondrial gene content or feature counts falling outside the 2.5th–97.5th percentiles. After standard preprocessing and normalization, datasets were first integrated across samples using the Seurat anchor-based integration workflow. Myeloid-derived cell populations were subsetted from the integrated datasets based on canonical marker expression (for example, CD14 and LYZ) and further analyzed independently. To further refine clustering within the myeloid compartment and mitigate residual batch effects, Harmony[61] (version 1.2.3) was applied to the myeloid subset prior to dimensionality reduction, clustering and visualization. Lineage-specific identities were assigned using a combination of SingleR[62] (version 2.10.1) and manual curation based on canonical marker gene expression. Pathway activity was assessed using gene set enrichment analysis (GSEA, version 4.4.0), and AUCell (version 1.30.1) was used to calculate gene set scores at the single-cell level[63].

Three M1-associated gene sets were used to characterize M1 macrophages. The Jablonski_M1_top50 (ref. 46) included the following genes: *Ms4a4c*, *Fpr2*, *Cxcl9*, *Lcn2*, *Cd38*, *Il12b*, *Fpr1*, *Cxcl10*, *Slfn4*, *Cfb*, *Il1b*, *Il1a*, *Ifit1*, *Gbp6*, *Ifit2*, *Slfn1*, *Gpr31b*, *Ptges*, *Ifit3*, *Oasl1*, *Zfp811*, *Rsad2*, *Isg20*, *Adgb*, *Fscn1*, *Cd200*, *Cxcl11*, *Ptgs2*, *Il6*, *Ifi44*, *Il12a*, *Socs3*, *Ifit1bl1*, *Acsl1*, *Ifi213*, *Marco*, *Cxcl3*, *Antxr1*, *Saa3*, *Gpr18*, *Clec4e*, *Hp*, *Irf7*, *Ccrl2*, *Klra2*, *Spic*, *Serpinb2*, *Plpp1*, *Smpdl3b* and *Ccr7*. The Buscher_M1_top50 (ref. 64) included the following genes: *Irg1*, *Cd40*, *Ptgs2*, *Ccl2*, *Csf2*, *Marcksl1*, *Il12a*, *Il12b*, *Icam1*, *Ifit2*, *Il23a*, *Vcam1*, *Rsad2*, *Cmpk2*, *Gpr84*, *Nfkbiz*, *Rtp4*, *Ehd1*, *Traf1*, *Ccnd2*, *Socs3*, *Adora2a*, *Slc7a11*, *Maff*, *Cish*, *Ccl7*, *Ccl22*, *Serpine1*, *Serpinb2*, *Slfn1*, *Cd38*, *Inhba*, *Edn1*, *Csf1*, *Lcn2*, *Mefv*, *Aqp9*, *Gpr85*, *Nfkb2*, *Pde4b*, *Hbegf*, *Trex1*, *AW112010*, *Il15ra*, *Ier3*, *Ifi47*, *Nfkbie*, *Oasl2*, *Irf7* and *Zbp1*. The THP1_M1_top50 (ref. 65) included the following genes: *TJP1*, *FPR2*, *WASF4P*, *EBI3*, *WARS*, *MX2*, *PCDH17*, *IFI27*, *COL15A1*, *EBLN2*, *FAM167A*, *PNPT1P1*, *HES4*, *CECR2*, *DDR1*, *CACNA2D1*, *TCP11L2*, *DDX58*, *ZNF224*, *ACTG1P3*, *FTH1P10*, *HIPK3*, *snoU13*, *SPRY1*, *CD274*, *CACHD1*, *TNFAIP3*, *OAS3*, *TAGAP*, *HCAR2*, *TH1P21*, *RAB39A*, *IGDCC4*, *CXCL2*, *KIF27*, *HNF4G*, *AKAP2*, *FAM20A*, *HK2P1*, *TRIO*, *C1R*, *MAP2K6*, *MAPK6PS4*, *TRANK1*, *APOL3*, *ADAM28*, *MX1*, *SAMD9L* and *EGF*.

Plasma protein profiling by Olink proximity extension assay

Peripheral blood samples were collected and centrifuged at 200*g* for 10 minutes to obtain PRP. The PRP fraction was subsequently centrifuged at 1,000*g* for 10 minutes to deplete residual platelets, and the resulting platelet-depleted plasma was aliquoted and stored at −80 °C until analysis. Prior to analysis, samples were thawed on ice and diluted according to the manufacturer's protocols.

Protein quantification was performed using the Olink Target 96 Immuno-Oncology panel (Olink Proteomics), which employs proximity extension assay (PEA) technology. In brief, samples were loaded into a 96-well plate and incubated with PEA probes, each consisting of a pair of oligonucleotide-labeled antibodies targeting specific proteins. Upon simultaneous binding to a target, the probes were brought into proximity, enabling a DNA polymerase-mediated extension event that generated unique DNA barcodes. These barcodes were subsequently amplified using quantitative real-time PCR, ensuring high sensitivity and specificity for protein detection. Data were normalized and quality controlled according to the manufacturer's recommendations.

Treatment protocols in the passive ITP model

BALB/c mice with antibody-induced ITP were treated with daily intraperitoneal injections starting on day 1 after induction. Treatment groups received either the CD38 inhibitor 78c at 50 mg kg^{-1} or NMN at 500 mg kg^{-1} once daily at approximately the same time each day. On day 6, peripheral blood was collected from the tail vein prior to euthanasia for immunoglobulin measurements. Blood was centrifuged at 200*g* for 10 minutes to obtain PRP; the PRP was then centrifuged at 1,000*g* for 10 minutes to remove residual platelets and stored at −80 °C until analysis. Mice were euthanized on day 6 for collection of spleens and subsequent downstream analyses.

Western blotting for NF-κB p65 phosphorylation

Differentiated mouse BMDMs were seeded in six-well plates at 3×10^5 cells per milliliter (3 ml per well) in IMDM supplemented with 10% FBS. After 12 hours of adherence, cells were serum starved overnight in serum-free IMDM and then treated with NMN (200 μg ml^{-1}) or vehicle control for 2 hours. Cells were then pretreated with betulinic acid (10 μM; MedChemExpress, HY-10529) or vehicle (DMSO) for 30 minutes, followed by stimulation with LPS (30 ng ml^{-1}) for an additional 30 minutes. After two washes with ice-cold PBS, cells were lysed in RIPA buffer (Beyotime Biotechnology, P0013B) containing protease and phosphatase inhibitors (Beyotime Biotechnology, P1045). Equal amounts of total protein were subjected to sodium dodecyl-sulfate polyacrylamide gel electrophoresis (SDS-PAGE), transferred to polyvinylidene fluoride (PVDF) membranes and immunoblotted with antibodies against total NF-κB p65 (clone D14E12; Cell Signaling Technology, 8242S, 1:500) and phospho-NF-κB p65 (Ser536) (Cell Signaling Technology, 3031S, 1:500). β-actin (clone 3H6G5; Servicebio, GB12001-100, 1:3,000) was used as a loading control. After incubation with HRP-conjugated secondary antibodies for 1 hour at room temperature, signals were visualized using enhanced chemiluminescence.

Assessment of NF-κB-mediated effects on macrophage polarization

To investigate NF-κB-mediated regulation of macrophage polarization, differentiated mouse BMDMs were plated at 3×10^5 cells per milliliter in IMDM containing 10% FBS in 24-well plates (1 ml per well). After overnight adherence, the cells were stimulated with LPS (30 ng ml^{-1}) under three conditions: (1) vehicle control, (2) NMN (200 μg ml^{-1}) or (3) NMN (200 μg ml^{-1}) plus betulinic acid (10 μM). NMN and betulinic acid were added at the start of LPS stimulation and maintained throughout the 72-hour incubation. Cells were collected using Accutase and subjected to flow cytometric analysis of M1 and M2 macrophage markers.

NLRP3 inflammasome assays

To evaluate NLRP3 inflammasome priming and activation, BMDMs were plated at 3×10^5 cells per milliliter in IMDM containing 10% FBS and allowed to adhere for 12 hours. The medium was replaced with IMDM containing 2% FBS, and NMN (200 μg ml^{-1}) or vehicle control was added immediately for a 16-hour pretreatment. For NLRP3 expression and IL-1β release assays, cells were seeded in 24-well plates at 1 ml per well. For caspase-1 activity assays, cells were seeded in six-well plates at 3 ml per well. After NMN/vehicle pretreatment, BMDMs were primed with LPS (30 ng ml^{-1}) for 6 hours at 37 °C.

NLRP3 expression. Immediately after the 6-hour LPS priming period (without nigericin stimulation), cells were washed with ice-cold PBS and lysed in NP-40 lysis buffer (Beyotime Biotechnology, P0013F) supplemented with a protease inhibitor cocktail. Clarified lysates were collected after centrifugation, and NLRP3 protein levels were quantified using a commercial ELISA kit (CUSABIO, CSB-EL015871MO) according to the manufacturer's instructions.

Caspase-1 activity. After 6-hour LPS priming, BMDMs were stimulated with nigericin (10 μM) for 30 minutes and then lysed, and caspase-1 activity in cell lysates was measured using a commercial caspase-1 activity assay kit (Beyotime Biotechnology, C1101) following the manufacturer's protocol.

IL-1β release. After 6-hour LPS priming, BMDMs were stimulated with nigericin (10 μM), and culture supernatants were collected 90 minutes after nigericin stimulation. Supernatants were cleared by centrifugation to remove debris, and IL-1β concentrations were determined by ELISA (NeoBioscience Technology, EMC001b) according to the manufacturer's instructions.

Induction of MDMs

PBMCs were isolated and seeded in six-well plates at 3×10^6 cells per well in complete RPMI 1640 medium for adherence. After 2 hours of incubation at 37 °C, non-adherent cells were removed by gentle PBS washing. Adherent monocytes were cultured in complete RPMI 1640 medium supplemented with 50 ng ml^{-1} recombinant human macrophage colony-stimulating factor (M-CSF) (R&D Systems, 216-MC) for 6 days, with half-medium changes every 3 days to induce differentiation into MDMs.

Macrophage polarization assays and flow cytometry

To assess the effects of CD38 blockade, knockout and NAD^+ replenishment on macrophage polarization, mouse BMDMs and human MDMs were plated at 3×10^5 cells per milliliter in IMDM or RPMI 1640 containing 10% FBS in 24-well plates (1 ml per well). After overnight adherence, the cells were stimulated with LPS (30 ng ml^{-1}) for 72 hours. For BMDMs, cells were cultured in the presence or absence of NMN (200 μg ml^{-1}). For MDMs, cells were cultured in the presence or absence of NMN (200 μg ml^{-1}) or a humanized anti-CD38 mAb (2 μg ml^{-1}; Keymed Biosciences, CM313). Treatments were added at the start of LPS stimulation and maintained throughout the incubation period. At the end of stimulation, adherent cells were harvested using Accutase and processed into single-cell suspensions for flow cytometry. In addition, splenic single-cell suspensions from ITP mice were prepared and analyzed in parallel to quantify in vivo macrophage polarization using the similar antibody panel and workflow described below.

For mouse splenic macrophage analysis, splenic single-cell suspensions were adjusted to 2×10^7 cells per milliliter, and 100 μl was used for staining. After Fc receptor blockade, samples were incubated with fluorochrome-conjugated antibodies for 15 minutes at room temperature in the dark, washed with PBS and fixed before acquisition. The following antibodies were used: APC-conjugated anti-F4/80, PE-Cy7-conjugated anti-CD11b, BV510-conjugated anti-CD86 (clone GL1; BioLegend, 105040) and PE-conjugated anti-CD206 (clone C068C2; BioLegend, 141706). For BMDM macrophage analysis, 3×10^5 detached BMDMs were resuspended in 100 μl of PBS for staining. After Fc receptor blockade, cells were incubated with APC-conjugated anti-F4/80, BV510-conjugated anti-CD86 and PE-conjugated anti-CD206 for 15 minutes at room temperature in the dark, washed with PBS and fixed before acquisition.

For human MDMs, 100 μl of single-cell suspensions (3×10^5 cells) were stained with surface antibodies for 15 minutes at room temperature in the dark, including BV510-conjugated anti-CD86 (clone IT2.2; BioLegend, 305432) and PE-conjugated anti-CD206 (clone 15-2; BioLegend, 321106). Cells were then fixed and permeabilized using a Fixation/Permeabilization Solution Kit (BD Biosciences, 554714) according to the manufacturer's instructions, followed by intracellular staining with APC-conjugated anti-CD68 (clone Y1/82A; BioLegend, 333810) for 30 minutes at room temperature. Cells were washed with PBS and fixed prior to acquisition.

All samples were acquired on a FACSCanto II (BD Biosciences) or a FongCyte flow cytometer, and data were analyzed using FlowJo version 10.0. The gating strategy is shown in Supplementary Fig. 10.

Cytokine quantification in macrophage cultures and patient plasma by ELISA

For cytokine measurements under NAD^+-modulating conditions, differentiated mouse BMDMs were plated at 3×10^5 cells per milliliter in IMDM containing 10% FBS in 24-well plates (1 ml per well). After overnight adherence, the cells were stimulated with LPS (30 ng ml^{-1}) for 72 hours in the presence or absence of NMN (200 µg ml^{-1}). Culture supernatants were collected 72 hours after LPS stimulation for quantification of cytokines and stored at −80 °C until analysis.

In addition, peripheral blood samples were collected from participants enrolled in the oral NMN clinical trial at baseline (pretreatment) and after 2 weeks of NMN administration, and platelet-depleted plasma was prepared as described above and stored at −80 °C until analysis.

Samples were thawed on ice and diluted to fall within the linear range of the assays. Concentrations of TNF (EMC102a.96 for mouse, EHC103a.96 for human; NeoBioscience Technology), IL-6 (EMC004.96 for mouse; NeoBioscience Technology), IFNγ (EHC102g.96 for human; NeoBioscience Technology) and iNOS (E-EL-M0696 for mouse, E-EL-H0753 for human; Elabscience) were measured using commercial ELISA kits according to the manufacturers' instructions.

Quantification of NAD^+ and NADH

Intracellular NAD^+ and NADH levels were measured using a NAD^+/NADH Detection Kit based on the WST-8 colorimetric method (Beyotime Biotechnology, S0175) following the manufacturer's instructions.

For mouse BMDMs, cells were seeded in six-well plates at 1×10^6 cells per well and allowed to adhere for 12 hours. Cells were then treated with NMN (200 µg ml^{-1}) or vehicle and stimulated with LPS (30 ng ml^{-1}) for 16 hours, after which NAD^+/NADH was quantified. For human MDMs, cells were treated with anti-CD38 mAb (2 µg ml^{-1}) or NMN (200 µg ml^{-1}) and stimulated with LPS (30 ng ml^{-1}) for 16 hours prior to NAD^+/NADH measurement.

For baseline samples from the oral NMN clinical trial, PBMCs were isolated as described above, and NAD^+/NADH was measured using 1×10^6 PBMCs per sample.

Approximately 1×10^6 cells were lysed in 200 µl of extraction buffer by gently pipetting. Lysates were centrifuged at 10,000*g* for 10 minutes at 4 °C, and the supernatant was collected for analysis. For total NAD^+/NADH measurement, a 20-µl aliquot of lysate was transferred to a 96-well plate, mixed with 90 µl of ethanol dehydrogenase working solution and incubated at 37 °C in the dark for 10 minutes. Subsequently, 10 µl of color reagent was added and incubated for an additional 10 minutes. Absorbance was measured at 450 nm using a Synergy H4 microplate reader (BioTek). To normalize across samples, measured concentrations were scaled to the equivalent concentration for 1×10^6 cells lysed in 200 µl.

To quantify NADH alone, samples were heated at 60 °C for 30 minutes to degrade NAD^+, followed by centrifugation at 10,000*g* for 10 minutes at 4 °C to remove insoluble material. The supernatant was then subjected to the same detection procedure. NAD^+ concentrations were calculated by subtracting the NADH values from the total NAD^+/NADH levels.

In vitro platelet phagocytosis assay

After the indicated LPS stimulation (30 ng ml^{-1}) with or without NMN (200 µg ml^{-1}) or anti-CD38 mAb (2 µg ml^{-1}) for 72 hours, BMDMs or MDMs were co-cultured with CFSE (Thermo Fisher Scientific, C34554)-labeled, anti-CD41 mAb (anti-mouse CD41, clone MWReg30; BioLegend, 133902 for BMDM and anti-human CD41, clone HIP8; BioLegend, 303702 for MDM) opsonized platelets (prepared using the same labeling and opsonization conditions as in the in vivo platelet clearance assay, as described above) at a 1:10 ratio (macrophages to platelets) for 2 hours at 37 °C in a humidified 5% CO_2 incubator. After incubation, extracellular fluorescence was quenched with 0.1% Trypan Blue for 2 minutes, followed by thorough washing with PBS. Cells were detached using Accutase, stained with APC-conjugated anti-F4/80 or anti-CD68 for 15–30 minutes at room temperature and analyzed by FACSCanto II. Macrophages were gated based on FSC/SSC and APC positivity, and phagocytic activity was quantified within the gated population as the Phagocytic Index, defined as:

$$\text{Phagocytic Index} = \text{Mean Fluorescence Intensity (MFI) of CFSE} \times \text{Percentage of CFSE}^+ \text{ macrophages}$$

Flow cytometry for FcγRI expression

Differentiated mouse BMDMs or human MDMs were plated at 3×10^5 cells per milliliter in IMDM or RPMI 1640 supplemented with 10% FBS in 24-well plates (1 ml per well). After 12 hours of adherence, the medium was replaced with IMDM or RPMI 1640 containing 2% FBS, and NMN (200 µg ml^{-1}) or anti-CD38 mAb (2 µg ml^{-1}) was added immediately for a 16-hour pretreatment. Cells were then stimulated with LPS (30 ng ml^{-1}) for 24 hours in the continued presence of NMN or anti-CD38 mAb. Adherent cells were detached using Accutase, washed and resuspended in 100 µl of PBS.

For mouse Fcγ receptor profiling, cells were incubated with fluorochrome-conjugated surface antibodies (APC-conjugated anti-F4/80 and BV421-conjugated anti-CD64 (clone X54-5/7.1; BioLegend, 139309)) for 15 minutes at room temperature in the dark, washed twice with PBS and fixed prior to acquisition. For human MDMs, cells were stained with BV421-conjugated anti-CD64 (clone 10.1; BioLegend, 305020) for 15 minutess at room temperature in the dark and then fixed and permeabilized using Fixation/Permeabilization solution, washed twice with wash buffer and incubated with APC-Cy7-conjugated anti-CD68 (clone Y1/82A; BioLegend, 333822) for 30 minutes at room temperature. After two final PBS washes, cells were fixed and analyzed by flow cytometry.

OVA immunization and assessment of humoral immune responses

To evaluate whether NMN supplementation affects humoral immunity, mice received NMN (500 mg kg^{-1}, intraperitoneal injection) starting on day −3 and administered once daily thereafter until euthanasia. On day 0, mice were immunized intraperitoneally with OVA (50 µg) formulated with Alhydrogel adjuvant 2% (InvivoGen, vac-alu-50). In brief, OVA was dissolved in 100 µl of PBS and mixed 1:1 (v/v) with Alhydrogel by gentle inversion for 15–30 minutes at room temperature to facilitate antigen adsorption, followed by intraperitoneal injection.

Peripheral blood was collected from the tail vein on day −3, day 7 and day 14 to quantify OVA-specific IgM and on day −3, day 14 and day 21 to quantify OVA-specific IgG. Peripheral blood was collected from the tail vein into EDTA anticoagulant and centrifuged at 200*g* for 10 minutes to obtain PRP. The PRP was further centrifuged at 1,000*g* for 10 minutes to remove platelets and stored at −80 °C until analysis. On day 21, mice were euthanized, and spleens were harvested for flow cytometric assessment of GCB cells.

Flow cytometric analysis of B cell subsets

For mouse plasma cell analysis, 100 µl of splenic single-cell suspensions (2×10^7 cells per milliliter) were stained with FITC-conjugated anti-CD19 (clone 1D3/CD19; BioLegend, 152403), BV510-conjugated anti-CD138 (clone 281-2; BioLegend, 142521) and PE-conjugated anti-IgD (clone 11-26c.2a; BioLegend, 405705). For GCB cell analysis, splenic single-cell suspensions were stained with FITC-conjugated anti-B220 (clone RA3-6B2; BioLegend, 103205), APC-conjugated anti-GL7 (clone GL7; BioLegend, 144617) and PE-conjugated anti-Fas (clone SA367H8; BioLegend, 152607). Cells were incubated with fluorochrome-conjugated surface antibodies for 15 minutes at room temperature in the dark, washed twice with PBS and fixed prior to acquisition.

For human B cell subset analysis, 100 µl of whole peripheral blood from patients with ITP was incubated with FITC-conjugated

anti-CD19 (clone HIB19; BioLegend, 302205), APC-Cy7-conjugated anti-CD138 (clone MI15; BioLegend, 356527), PE-Cy7-conjugated anti-IgD (clone W18340F; BioLegend, 307811) and BV421-conjugated anti-CD27 (clone M-T271; BioLegend, 356417) for 15 minutes at room temperature in the dark. Red blood cells were then lysed using lysing buffer (BD Biosciences, 555899) for 5 minutes at room temperature, followed by washing with PBS. Cells were fixed prior to acquisition. All samples were acquired on a FongCyte flow cytometer, and data were analyzed using FlowJo version 10.0. The gating strategy is shown in Supplementary Fig. 11.

Quantification of total plasma immunoglobulins and OVA-specific antibodies

Platelet-poor plasma (PPP) was used for ELISA-based quantification of total mouse IgM (Beyotime Biotechnology, PI489), IgA (Beyotime Biotechnology, PI471) and IgG (Beyotime Biotechnology, PI480), as well as OVA-specific IgM (Chondrex, 3017) and IgG (Chondrex, 3011), using the corresponding commercial ELISA kits according to the manufacturers' instructions.

Flow cytometric analysis of CD38, CD86 and CD206 expression on monocytes

Peripheral blood was collected from patients before NMN treatment. For staining, two tubes of 100 µl of whole blood per sample were prepared. One tube was incubated with APC-conjugated anti-CD14 (clone M5E2; BioLegend, 301807) and PE-conjugated anti-CD38 (clone HIT2; BioLegend, 303506). The other tube was incubated with APC-conjugated anti-CD14, PE-Cy7-conjugated anti-CD86 (clone IT2.2; BioLegend, 305422) and PE-conjugated anti-CD206 (clone 15-2; BioLegend, 321106) for 15 minutes at room temperature in the dark. Red blood cells were then lysed using lysing buffer for 5 minutes at room temperature, followed by washing with PBS. Cells were fixed before acquisition. Samples were acquired on a FongCyte flow cytometer, and data were analyzed using FlowJo version 10.0. The gating strategy is shown in Supplementary Fig. 12.

Platelet activation and aggregation

Human PRP was used to assess the effects of NMN on platelet activation and aggregation. For mouse experiments, PRP was used for platelet activation analyses, whereas washed platelets were used for aggregation assays.

For human studies, peripheral blood was collected into sodium citrate anticoagulant tubes, and PRP was prepared by centrifugation of whole blood at 200*g* for 10 minutes at room temperature. PPP was generated from PRP and used to adjust PRP to 2×10^8 platelets per milliliter. For platelet activation, adjusted PRP was incubated with NMN (200 µg ml^{-1}) or vehicle at 37 °C for 30 minutes, stimulated with collagen (2 µg ml^{-1}; Helena Laboratories, 5368) at 37 °C for 5 minutes, quenched with EDTA (final 5 mM) on ice, stained with PE-conjugated anti-CD42b (clone HIP1; BioLegend, 303906) and APC-Cy7-conjugated anti-CD62P (clone AK4; BioLegend, 304944) for 20 minutes on ice, washed, fixed with 2% PFA and acquired by flow cytometry. For aggregation, adjusted PRP was incubated with NMN (200 µg ml^{-1}) or vehicle at 37 °C for 30 minutes and assessed by light transmission aggregometry (LTA) at 37 °C with stirring at 1,000 rpm after the addition of collagen (2 µg ml^{-1}). PPP was used as the reference (blank; 100% light transmission), and maximum aggregation within 5–10 minutes was recorded.

For mouse studies, blood was collected via the retro-orbital venous plexus into ACD and centrifuged at 200*g* for 10 minutes at room temperature to obtain PRP. For platelet activation, similarly to human PRP, mouse PRP was adjusted to 2×10^8 per milliliter and incubated with NMN (200 µg ml^{-1}) or vehicle at 37 °C for 30 minutes, stimulated with collagen (2 µg ml^{-1}) at 37 °C for 5 minutes, quenched with EDTA (final 5 mM) on ice and stained with FITC-conjugated anti-CD41 (clone MWReg30; BioLegend, 133903) and APC-conjugated anti-CD62P (clone RMP-1; BioLegend, 148303) for 20 minutes on ice in the dark, followed by washing, fixation and flow cytometric acquisition. All samples were acquired on a FongCyte flow cytometer, and data were analyzed using FlowJo version 10.0. The gating strategy is shown in Supplementary Fig. 13. For platelet aggregation assays, washed platelets were resuspended in prewarmed modified Tyrode's buffer and adjusted to 2×10^8 platelets per milliliter. Ca^{2+} and Mg^{2+} were added to a final concentration of 1 mM each, and platelets were rested for 1 hour at room temperature. Platelets were then incubated with NMN (200 µg ml^{-1}) or vehicle at 37 °C for 30 minutes. Aggregation was measured by LTA at 37 °C with stirring at 1,000 r.p.m. after the addition of collagen (2 µg ml^{-1}). Modified Tyrode's buffer was used as the reference (blank; 100% light transmission), and maximum aggregation was recorded within 5–10 minutes.

Statistical analysis

Statistical analyses were performed using SPSS version 24.0 (IBM) and GraphPad Prism version 8.0 (GraphPad Software). For the clinical trial results, quantitative variables are summarized as median (IQR), and categorical variables are presented as frequency (percentage). For mechanistic experiments, data are presented as mean ± s.e.m. unless otherwise stated. Unless otherwise specified, measurements represent biological replicates from distinct individuals/samples (independent observations). For experiments with repeated measurements over time, the same subjects were measured repeatedly (paired/repeated measures).

For comparisons between two groups, the Mann–Whitney *U*-test was used for unpaired data and the paired Wilcoxon signed-rank test for paired data, as appropriate. For longitudinal data with repeated measurements over time, we used a two-way repeated-measures ANOVA with genotype/treatment as the between-subject factor and time as the within-subject factor. When sphericity was violated, the Geisser–Greenhouse correction was applied (GraphPad Prism). No post hoc comparisons at individual timepoints were performed unless otherwise stated. Unless otherwise stated, the main *P* values reported in the figures correspond to the main effect of group (genotype/treatment) across the timecourse. When more than two groups are displayed, *P* values are derived from prespecified pairwise comparisons as stated in the figure legends. All statistical tests were two-sided, and a two-sided $P < 0.05$ was considered statistically significant.

Declaration of generative AI and AI-assisted technologies in the writing process

During the preparation of this work, the authors used ChatGPT 5.0 to improve language and readability. After using this tool, the authors reviewed and edited the content as needed and take full responsibility for the content of the published article.

Reporting summary

Further information on research design is available in the Nature Portfolio Reporting Summary linked to this article.

Data availability

Raw sequencing data have been deposited in the Genome Sequence Archive of the National Genomics Data Center (Beijing, China) under HRA009819, HRA002792 and CRA026219. The data deposited and made public are compliant with the regulations of the Ministry of Science and Technology of China.

Deidentified individual participant-level efficacy and immune monitoring data underlying the main findings, together with the study protocol, statistical analysis plan and data dictionary, are provided in Supplementary Information. Additional deidentified participant-level data not included in the article may be made available to qualified academic investigators for non-commercial research purposes, subject to institutional review and applicable ethical and legal requirements. Requests should be directed to the corresponding author (zhanglei1@ihcams.ac.cn) and

will be reviewed within 4 weeks. Approved requests may require a data access agreement. Source data are provided with this paper.

References

58. Neunert, C. et al. American Society of Hematology 2019 guidelines for immune thrombocytopenia. *Blood Adv.* **3**, 3829–3866 (2019).
59. Katsman, Y., Foo, A. H., Leontyev, D. & Branch, D. R. Improved mouse models for the study of treatment modalities for immune-mediated platelet destruction. *Transfusion* **50**, 1285–1294 (2010).
60. Stuart, T. et al. Comprehensive integration of single-cell data. *Cell* **177**, 1888–1902 (2019).
61. Korsunsky, I. et al. Fast, sensitive and accurate integration of single-cell data with Harmony. *Nat. Methods* **16**, 1289–1296 (2019).
62. Aran, D. et al. Reference-based analysis of lung single-cell sequencing reveals a transitional profibrotic macrophage. *Nat. Immunol.* **20**, 163–172 (2019).
63. Aibar, S. et al. SCENIC: single-cell regulatory network inference and clustering. *Nat. Methods* **14**, 1083–1086 (2017).
64. Buscher, K. et al. Natural variation of macrophage activation as disease-relevant phenotype predictive of inflammation and cancer survival. *Nat. Commun.* **8**, 16041 (2017).
65. He, L. et al. Global characterization of macrophage polarization mechanisms and identification of M2-type polarization inhibitors. *Cell Rep.* **37**, 109955 (2021).

Acknowledgements

We thank J. Tao for providing the *Cd38*KO mice. This work was supported by grants from the National Natural Science Foundation of China (82570173 to H.L., 82470136 to R.Y. and 82341214 to J.W.); the National Key Research and Development Program of China (2023YFC2507802 to F.X.); the CAMS Innovation Fund for Medical Sciences (2024-I2M-ZH-016 to L.Z. and 2025-I2M-XHZY-034 to L.Z.); the Tianjin Municipal Science and Technology Commission (25ZXZSSS00510 to L.Z.); and the Distinguished Young Scholars of Tianjin (22JCJQJC00070 to J.W.).

Author contributions

H.L. and Yuan Xu performed the experiments, analyzed the data, created the figures and wrote the paper. Y. Chen was responsible for clinical trial design, execution and patient data collection and analysis. L.J. and Yanmei Xu performed the experiments and analyzed the data. W.Z. designed the study, assisted with experimental procedures and analyzed the data. T.S., R.F., X.L., F.X. and W.L. collected patient samples and participated in the clinical trial. X.P., W.W. and Y. Chi assisted with experimental procedures, including cell culture and animal experiments. R.Y. provided resources. J.W. designed and supervised the study, analyzed the data and wrote the paper. L.Z. designed and implemented the study, supervised experiments, analyzed the data, wrote the paper and provided resources.

Competing interests

The authors declare no competing interests.

Additional information

Extended data is available for this paper at https://doi.org/10.1038/s41591-026-04366-x.

Supplementary information The online version contains supplementary material available at https://doi.org/10.1038/s41591-026-04366-x.

Correspondence and requests for materials should be addressed to Jun Wei or Lei Zhang.

Peer review information *Nature Medicine* thanks Sebastian Vogel and the other, anonymous, reviewer(s) for their contribution to the peer review of this work. Primary Handling Editor: Saheli Sadanand, in collaboration with the *Nature Medicine* team.

https://doi.org/10.1038/s41591-026-04366-x

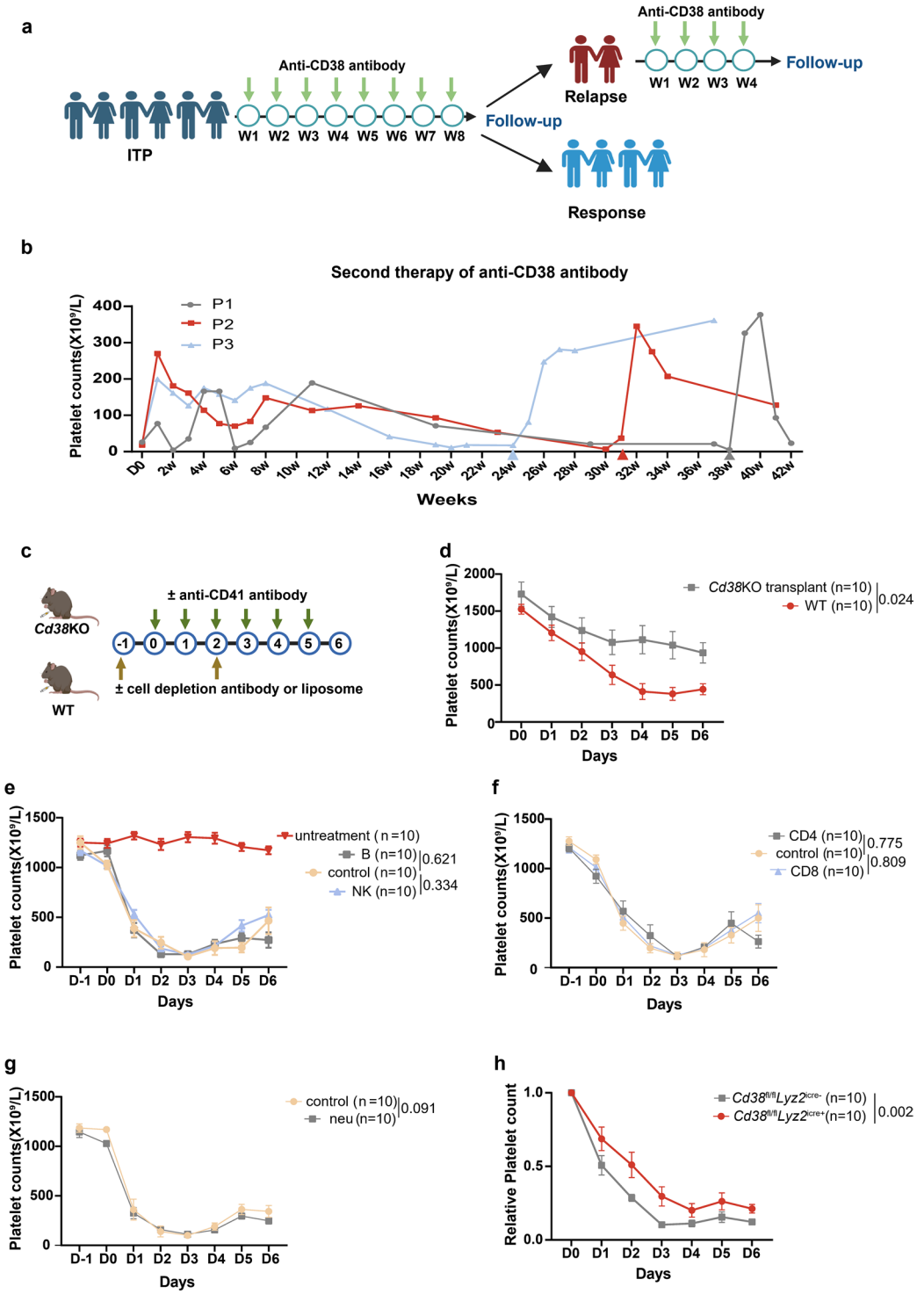

Extended Data Fig. 1 | CD38 deficiency in hematopoietic cells mitigates thrombocytopenia in passive ITP. **a**, Schematic overview of the clinical study design and follow-up protocol evaluating anti-CD38 monoclonal antibody (mAb) therapy in patients with refractory immune thrombocytopenia (ITP). **b**, Platelet recovery kinetics in three ITP patients from initial treatment to relapse and subsequent re-treatment with anti-CD38 mAb. Triangles mark the initiation of the second treatment. **c**, Experimental design for passive ITP induction and immune cell depletion in wild-type (WT) and *Cd38* knockout (*Cd38*KO) mice. **d**, Platelet count kinetics in WT recipient mice reconstituted with *Cd38*KO or WT bone marrow cells, after hematopoietic reconstitution and passive ITP induction (n = 10 per group). **e**, Daily platelet counts in WT mice following depletion of B cells or natural killer (NK) cells prior to ITP induction, including corresponding no ITP induction group and ITP group without cell depletion (n = 10 per group). **f**, Daily platelet counts in WT mice following depletion of $CD4^+$ or $CD8^+$ T cells prior to ITP induction, with a nondepleted WT ITP group as the control. (n = 10 per group). **g**, Daily platelet counts in WT mice following depletion of neutrophils (neu) prior to ITP induction, with a nondepleted WT ITP group as the control. (n = 10 per group). **h**, Relative platelet counts in myeloid-specific *Cd38*-deficient mice ($Cd38^{fl/fl}$; $Lyz2^{-iCre+}$) and $iCre^-$ littermate controls following passive ITP induction (n = 10 per group). Relative platelet counts were normalized to baseline (day 0 (D0)). Data are presented as mean ± s.e.m. Statistical analyses were restricted to prespecified pairwise comparisons using two-way repeated-measures ANOVA (**d**-**h**). Absence of *p*-value indicates that no comparison was performed. Panels **a** and **c** created in BioRender: **a**, Li, H. https://biorender.com/lkr78rd (2026); **c**, Li, H. https://biorender.com/84bz44p (2026).

https://doi.org/10.1038/s41591-026-04366-x

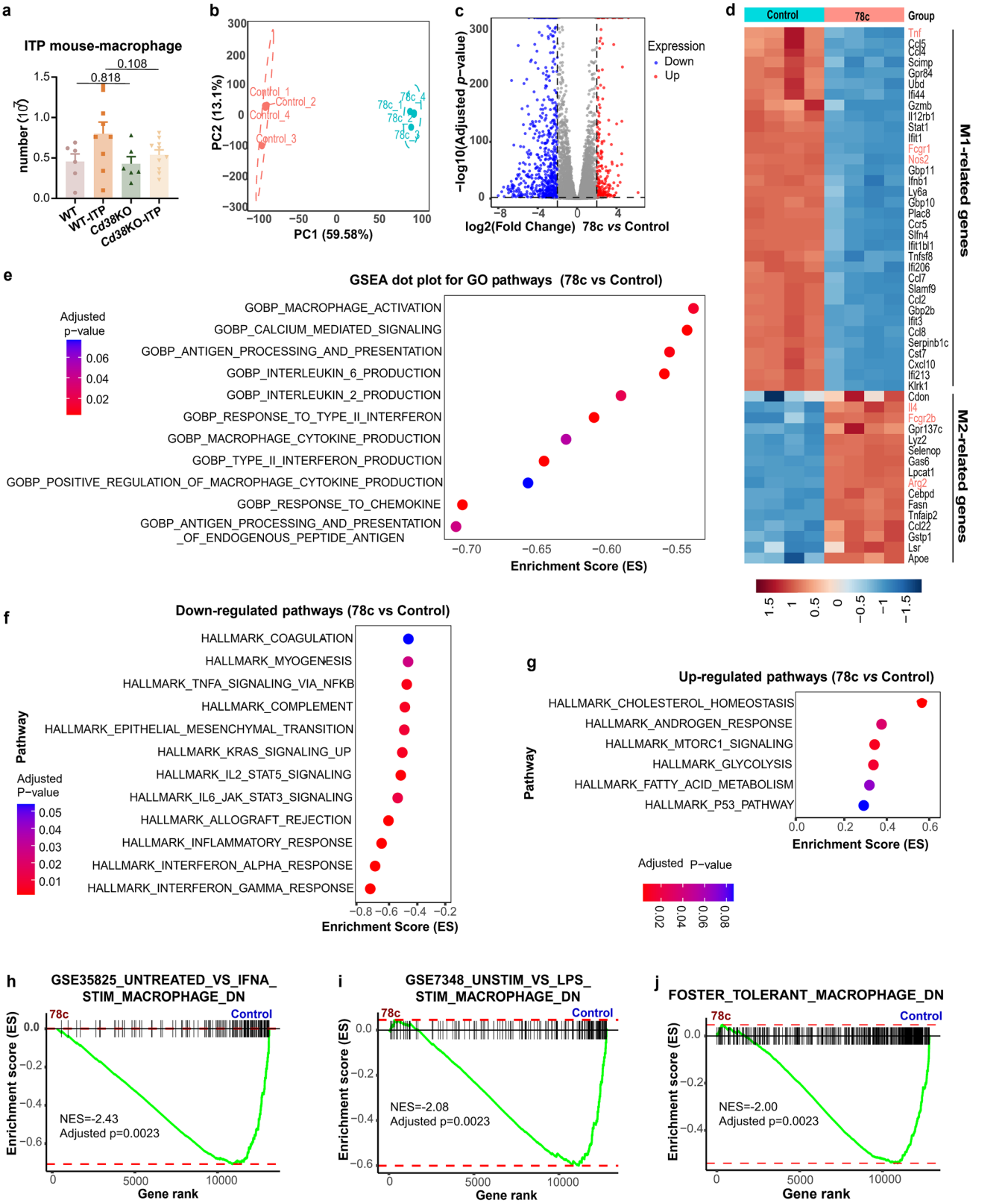

Extended Data Fig. 2 | See next page for caption.

https://doi.org/10.1038/s41591-026-04366-x

Extended Data Fig. 2 | Inhibition of CD38 enzymatic activity attenuates pro-inflammatory macrophage polarization. a, Flow cytometric quantification of splenic macrophages in wild-type (WT) and *Cd38* knockout (*Cd38*KO) mice with or without immune thrombocytopenia (ITP) (WT-ITP, n = 9; *Cd38*KO-ITP, n = 10; WT, n = 6; *Cd38*KO, n = 6). Data are presented as mean ± s.e.m. Statistical differences were assessed by two-sided Mann-Whitney U tests for prespecified pairwise comparisons. Absence of statistical annotation indicates that no comparison was performed. **b**, Principal component analysis (PCA) of transcriptomes from bone marrow-derived macrophages (BMDMs) treated with or without CD38 inhibitor 78c (n = 4 per group). **c**, Volcano plot showing differentially expressed genes (DEGs) between BMDMs with or without 78c treatment identified by DESeq2 using the two-sided Wald test, with p values adjusted for multiple comparisons by the Benjamini–Hochberg method. **d**, Heatmap of differentially expressed representative M1- and M2-associated genes in BMDMs with or without 78c treatment. **e**, Gene set enrichment analysis (GSEA) of Gene Ontology (GO) pathways in BMDMs following CD38 inhibition. **f**, GSEA of downregulated hallmark pathways in BMDMs following CD38 inhibition. **g**, GSEA of upregulated hallmark pathways in BMDMs following CD38 inhibition. **h-j**, GSEA enrichment plots of M1-associated gene sets in 78c-treated versus control BMDMs. Enrichment *p* values for GSEA analysis were estimated using the adaptive multilevel split Monte Carlo approach, and *p* values were adjusted for multiple comparisons using the Benjamini–Hochberg method.

https://doi.org/10.1038/s41591-026-04366-x

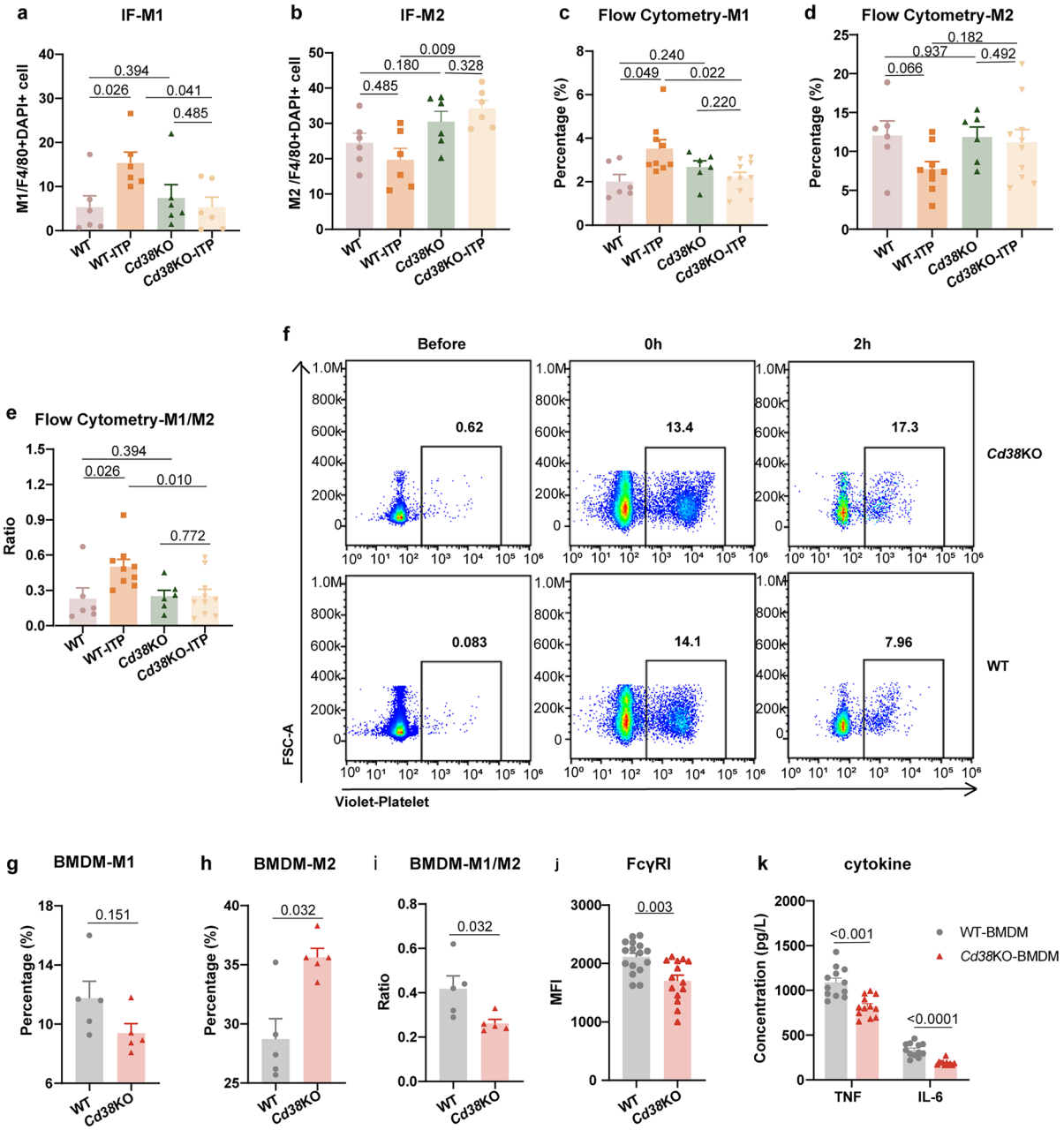

Extended Data Fig. 3 | CD38 deficiency reduces M1/M2 ratio, FcγRI expression and platelet destruction in ITP mice. a, b, Splenic proportion of M1 ($DAPI^+F4/80^+iNOS^+$) (**a**) and M2 ($DAPI^+F4/80^+CD163^+$) (**b**) macrophages detected by immunofluorescence (IF) staining in wild-type (WT) and *Cd38* knockout (*Cd38*KO) mice with or without immune thrombocytopenia (ITP) (n = 6 per group). **c, d**, Flow cytometry quantification of splenic M1 ($F4/80^+CD11b^{low}CD86^+CD206^-$) (**c**) and M2 ($F4/80^+CD11b^{low}CD86^-CD206^+$) (**d**) macrophages in WT and *Cd38*KO mice with or without ITP (WT-ITP, n = 9; *Cd38*KO-ITP, n = 10; WT, n = 6; *Cd38*KO, n = 6). **e**, Splenic M1/M2 macrophage ratio detected by flow cytometry across four groups (WT-ITP, n = 9; *Cd38*KO-ITP, n = 10; WT, n = 6; *Cd38*KO, n = 6). **f**, Representative flow cytometry plots showing circulating persistence of transfused fluorescently labeled opsonized platelets in WT and *Cd38*KO mice at indicated time points. **g, h**, Proportion of M1 (**g**) and M2 (**h**) macrophages in bone marrow–derived macrophages (BMDMs) from *Cd38*KO and WT mice detected by flow cytometry (n = 5 per group). **i**, M1/M2 macrophage ratio in BMDMs from *Cd38*KO and WT mice based on flow cytometric quantification (n = 5 per group). **j**, Surface Fc gamma receptor I (FcγRI) expression on WT and *Cd38*KO BMDMs, quantified as mean fluorescence intensity (MFI) by flow cytometry (WT, n = 16; *Cd38*KO, n = 14). **k**, Concentrations of TNF-α and IL-6 in culture supernatants of BMDMs from *Cd38*KO and WT (n = 12 per group) mice, measured by enzyme-linked immunosorbent assay (ELISA). Data are presented as mean ± s.e.m. Statistical differences were determined by two-sided Mann-Whitney U tests for prespecified pairwise comparisons. Absence of *p*-value indicates that no comparison was performed.

https://doi.org/10.1038/s41591-026-04366-x

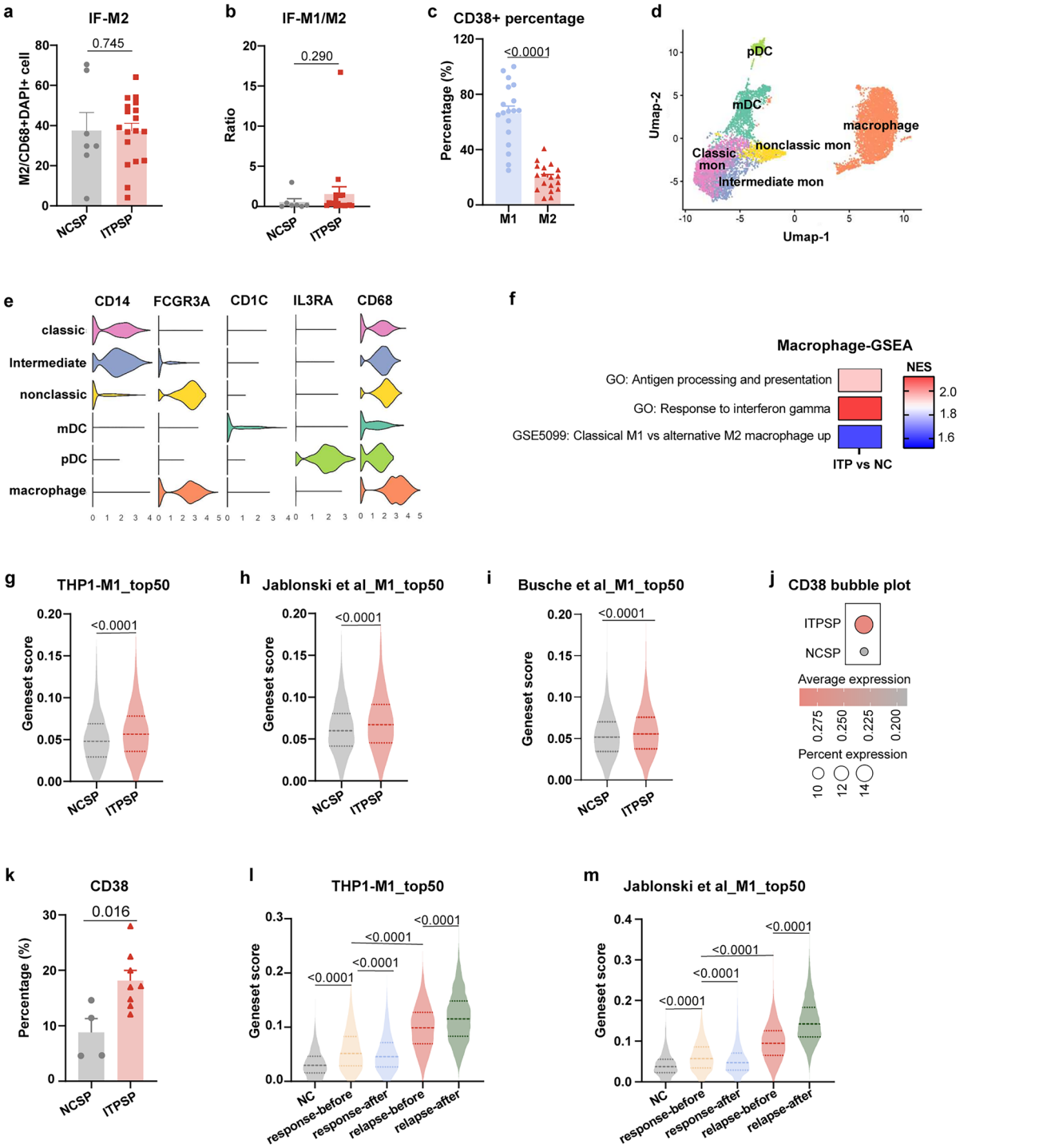

Extended Data Fig. 4 | Enhanced M1 polarization is reversed by anti-CD38 mAb in patients with ITP. a, Proportion of splenic M2 ($DAPI^+CD68^+CD163^+$) macrophages in immune thrombocytopenia (ITP) patients (n = 18) and trauma controls (n = 7), detected by immunofluorescence (IF) staining. NCSP, spleen from trauma controls; ITPSP, spleen from patients with ITP. **b**, Splenic M1/M2 ratio in ITP patients (n = 18) and trauma controls (n = 7) by IF. **c**, Proportion of $CD38^+$ cells among splenic M1 and M2 macrophages in ITP patients (n = 18) by IF. **d**, Unsupervised uniform manifold approximation and projection (UMAP) clustering of splenic myeloid-derived cells from single-cell sequencing (scRNA-seq) of ITP patients (n = 8) and trauma controls (n = 4). **e**, Violin plots showing expression of representative myeloid lineage marker genes in spleens from splenectomized ITP patients and trauma controls, by scRNA-seq. **f**, Gene set enrichment analysis (GSEA) of macrophage transcriptomes from ITP patients compared with trauma controls (NC). **g-i**, Single-cell transcriptomic analysis of M1-related gene set scores in splenic macrophages from ITP patients (n = 8) and trauma controls (n = 4). **j**, Bubble plot showing CD38 expression in splenic macrophages from ITP patients and trauma controls, by scRNA-seq. **k**, Proportion of $CD38^+$ macrophages among splenic macrophages in ITP patients (n = 8) and trauma controls (n = 4), by scRNA-seq. **l, m**, M1-related gene set scores in classical monocytes from normal controls (NC, n = 6), relapsed ITP patients (n = 4), and responders (n = 5) before and after anti-CD38 mAb therapy by scRNA-seq. Data are presented as mean ± s.e.m. (**a-c, k**) or median with interquartile range (**g-i, l** and **m**). Statistical differences were determined by two-sided Mann-Whitney U tests for prespecified pairwise comparisons. Absence of *p*-value indicates that no comparison was performed.

https://doi.org/10.1038/s41591-026-04366-x

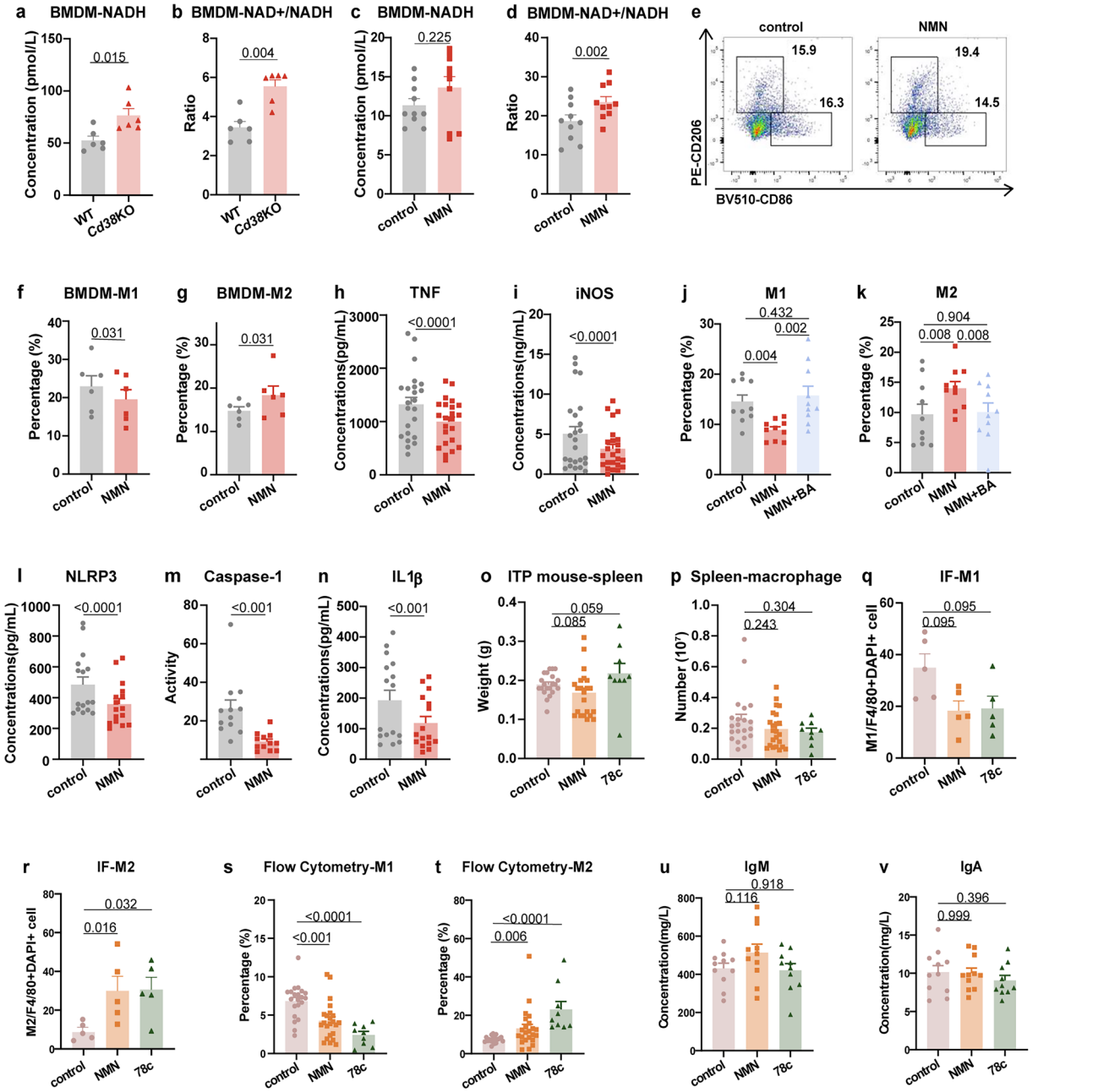

Extended Data Fig. 5 | NAD⁺ metabolism restrains inflammatory macrophage activation and preserves humoral immunity in ITP mice. a, b, NADH (**a**) and NAD⁺/NADH ratios (**b**) in bone marrow-derived macrophages (BMDMs) from *Cd38* knockout (*Cd38*KO) and wild-type (WT) mice (n = 6 per group). **c, d**, NADH (**c**) and NAD⁺/NADH ratios (**d**) in BMDMs with or without nicotinamide mononucleotide (NMN) (n = 10 per group). **e**, Representative plots of M1 and M2 in BMDMs with or without NMN. **f, g**, Quantification of M1 (**f**) and M2 (**g**) in BMDMs with or without NMN (n = 6 per group). **h,i**, TNF-α(**h**) and iNOS (**i**) in BMDMs supernatants with or without NMN (n = 23 per group). **j, k**, M1 (**j**) and M2 (**k**) proportions in BMDMs under control, NMN, or NMN plus betulinic acid (BA) (n = 10 per group). **l-n**, NOD-like receptor family, pyrin domain–containing 3 (NLRP3) protein abundance in lysates (**l**; n = 16 per group), caspase-1 activity (**m**; n = 12 per group) and IL-1β concentration in supernatants (**n**; n = 16 per group) of BMDMs with or without NMN. **o, p**, Spleen weight (**o**) and total splenic macrophage counts (**p**) in immune thrombocytopenia (ITP) mice receiving NMN (n = 23), 78c (n = 9), or vehicle (n = 21). **q-t**, Splenic M1 (**q, s**) and M2 (**r, t**) macrophages in ITP mice treated with NMN, 78c, or vehicle by immunofluorescence (IF) staining (n = 5 per group) and flow cytometry (n = 23 for NMN, n = 9 for 78c and n = 21 for vehicle). **u, v**, Plasma IgM (**u**) and IgA (**v**) in ITP mice receiving NMN (n = 11), 78c (n = 10), or vehicle (n = 11). Data are presented as mean ± s.e.m. Statistical differences were determined by two-sided Mann-Whitney U test (**a, b** and **o-v**) or two-sided Wilcoxon signed-rank test (**c**, **d** and **f-n**). Absence of *p*-value indicates that no comparison was performed.

https://doi.org/10.1038/s41591-026-04366-x

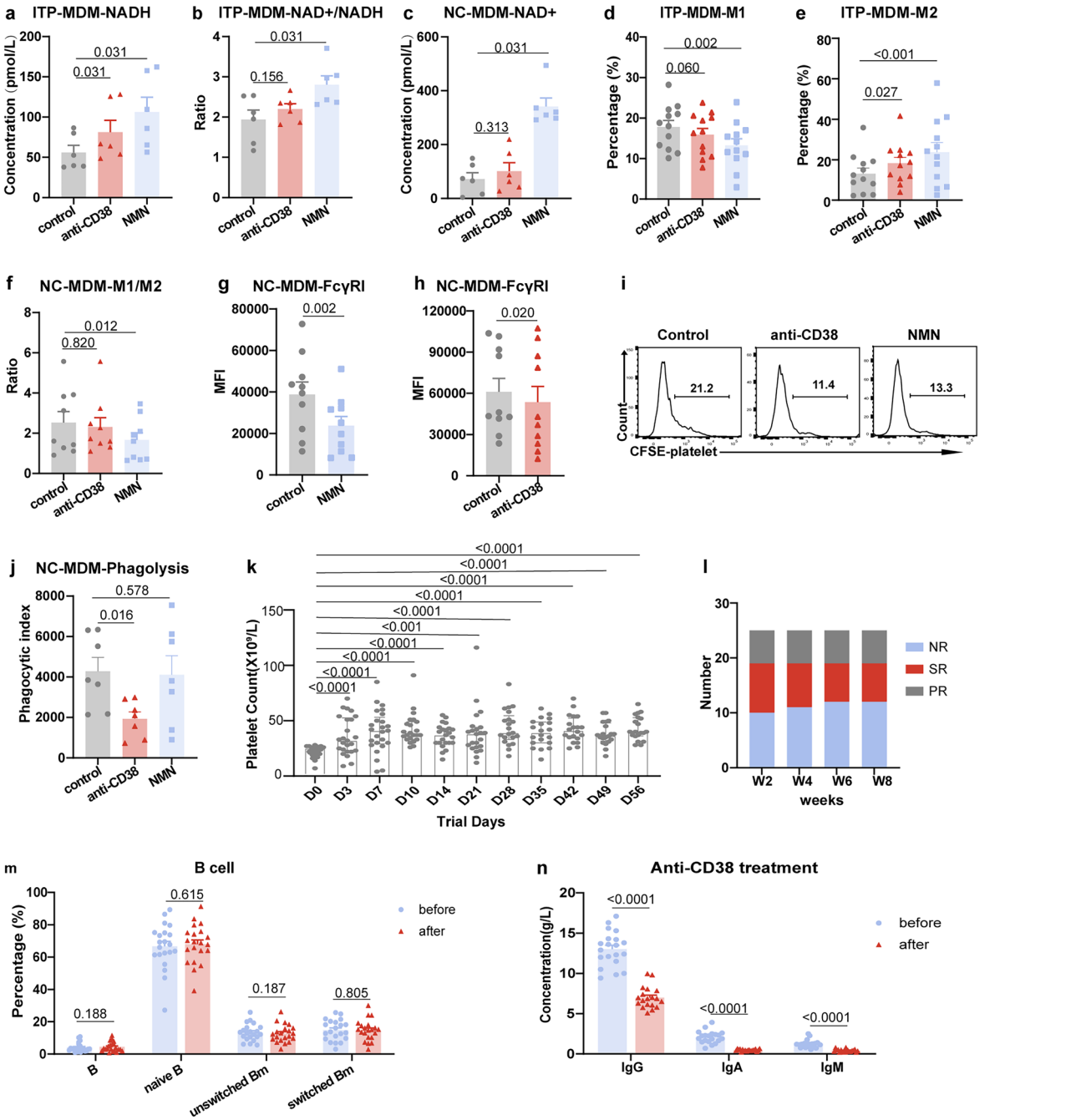

Extended Data Fig. 6 | NMN modulates macrophage phenotype and induces heterogeneous platelet responses in ITP patients. a, b, NADH (**a**) and NAD^+/NADH ratios (**b**) in monocyte-derived macrophages (MDMs) from immune thrombocytopenia (ITP) patients receiving vehicle, anti-CD38 monoclonal antibody (mAb) or nicotinamide mononucleotide (NMN) (n = 6 per group). **c**, NAD^+ in vehicle, anti-CD38 mAb- or NMN-treated MDMs from normal controls (NC) (n = 6 per group). **d, e**, M1 ($CD68^+CD86^+CD206^-$) (**d**) and M2 ($CD68^+CD86^-CD206^+$) (**e**) percentages in vehicle, anti-CD38 mAb- or NMN-treated MDMs from ITP patients (n = 12 per group). **f**, M1/M2 ratio in MDMs from NC treated with vehicle, anti-CD38 mAb or NMN (n = 9 per group). **g, h**, Fc gamma receptor I (FcγRI) expression on MDMs from NC treated with vehicle and NMN(**g**) or anti-CD38 mAb (**h**) (n = 10 per group), shown as mean fluorescence intensity (MFI). **i**, Representative flow cytometry plots showing platelet phagocytosis by MDMs from ITP patients treated with vehicle, anti-CD38 mAb or NMN. **j**, Platelet phagocytosis in MDMs from NC treated with vehicle, anti-CD38 mAb or NMN (n = 7 per group). **k**, Platelet counts over 8 weeks in all NMN-treated ITP patients (n = 25). **l**, Number of patients achieving partial response (PR), suboptimal response (SR) or no response (NR) over time (n = 25). **m**, Percentages of total B cells ($CD19^+$) within lymphocytes, naive ($CD19^+IgD^+CD27^-$), class-unswitched memory ($CD19^+IgD^+CD27^+$), and class-switched memory ($CD19^+IgD^-CD27^+$) B subsets within total B cells in ITP patients before and 8 weeks after NMN treatment (n = 21). **n**, Serum IgM, IgA, and IgG in ITP patients before and 8 weeks after anti-CD38 mAb treatment (n = 20). Data are presented as mean ± s.e.m. Statistical differences were determined by two-sided Wilcoxon signed-rank tests for prespecified paired comparisons. Absence of *p*-value indicates that no comparison was performed.

https://doi.org/10.1038/s41591-026-04366-x

Extended Data Table 1 | WHO bleeding score before and after treatment

Bleeding score	At enrollment (N=25), n (%)	At the end of Week 2 (N=25), n (%)
0	21 (84)	23 (92)
1	4 (16)	2 (8)
2	0 (0)	0 (0)
3	0 (0)	0 (0)
4	0 (0)	0 (0)

WHO bleeding scores after rescue therapy were treated as missing and imputed using last observation carried forward (LOCF) method if no bleeding occurred after rescue therapy, otherwise, the WHO bleeding score after rescue therapy was used for analysis.

WHO = World Health Organization.

https://doi.org/10.1038/s41591-026-04366-x

Extended Data Table 2 | Treatment-related adverse events in patients following anti-CD38 mAb treatment

	Patients (n = 21)				
Adverse event	Grade 1	Grade 2	Grade 3	Grade 4/5	Any Grade
	Number of patients (percent)				
Infusion-related reaction[a]	1 (4.8)	2 (9.5)	0 (0)	0 (0)	3 (14.3)
Upper respiratory tract infection	4 (19.0)	4 (19.0)	0 (0)	0 (0)	8 (38.1)
Neutropenia	1 (4.8)	0 (0)	0 (0)	0 (0)	1 (4.8)
Hyperuricemia	1 (4.8)	0 (0)	0 (0)	0 (0)	1 (4.8)

Note: All patients were followed for at least 24 weeks after the first infusion.

[a] One patient developed grade 1 rash. A second patient experienced grade 2 hypertension, chest discomfort, and dyspnea. A third patient presented with a grade 2 infusion-related reaction, characterized by chills, elevated blood pressure, chest discomfort or dyspnea, and blurred vision.

https://doi.org/10.1038/s41591-026-04366-x

Extended Data Table 3 | Baseline characteristics of patients with immune thrombocytopenia

Cohort	Sample size (n)	Sex, n (%) M / F	Age (year)	ITP duration (month)	Platelet count (×10⁹/L)
Anti-CD38 mAbs treated	21	4 (19.0) /17 (81.0)	41.0 (24.0–49.0)	48.0 (11.5–125.0)	12.0 (6.5–18.0)
Anti-CD38 mAbs retreated	3	0 (0) /3 (100.0)	25.0 (21.0–56.0)	72.0 (13–200)	16.0 (6.0–18.0)
Anti-CD38 mAbs scRNA-seq	9	2 (22.2) /7 (77.8)	39.0 (22.5–44.5)	20.0 (11.5–99.0)	8.0 (4.5–23.5)
Splenectomy for IF	18	2 (11.1) /16 (88.9)	50.5 (28.3–58.5)	66.0 (12.0–147.0)	6.5 (1.0–13.0)
Splenectomy for scRNA-seq	8	2 (25.0) /6 (75.0)	42.5 (21.5–57.3)	114.0 (9.0–195.0)	4.5 (2.3–12.5)
MDM induction	27	11 (40.7) /16 (59.3)	48.0 (29.0–55.0)	24.0 (3.0–96.0)	11.0 (5.0–20.0)

Note: Data are presented as median (IQR) or n (%).

n = number; IQR = interquartile range; M = male; F = female; MDMs = monocyte-derived macrophages; mAbs = Monoclonal antibodies; scRNA-seq = single-cell RNA sequencing; IF = immunofluorescence.

https://doi.org/10.1038/s41591-026-04366-x

Extended Data Table 4 | Concomitant medications used during the trial period

Patient no.	Concomitant medications at baseline	Concomitant medications after NMN
001	Prednisone 8 mg/d for 2 months	Prednisone therapy discontinued at week 4
024	Eltrombopag 75 mg/d for 1.5 months	No change

Note: NMN: nicotinamide mononucleotide

nature portfolio

Corresponding author(s): Lei Zhang

Last updated by author(s): Mar 19, 2026

Reporting Summary

Nature Portfolio wishes to improve the reproducibility of the work that we publish. This form provides structure for consistency and transparency in reporting. For further information on Nature Portfolio policies, see our Editorial Policies and the Editorial Policy Checklist.

Statistics

For all statistical analyses, confirm that the following items are present in the figure legend, table legend, main text, or Methods section.

n/a	Confirmed
☐	☒ The exact sample size (*n*) for each experimental group/condition, given as a discrete number and unit of measurement
☐	☒ A statement on whether measurements were taken from distinct samples or whether the same sample was measured repeatedly
☐	☒ The statistical test(s) used AND whether they are one- or two-sided *Only common tests should be described solely by name; describe more complex techniques in the Methods section.*
☒	☐ A description of all covariates tested
☒	☐ A description of any assumptions or corrections, such as tests of normality and adjustment for multiple comparisons
☐	☒ A full description of the statistical parameters including central tendency (e.g. means) or other basic estimates (e.g. regression coefficient) AND variation (e.g. standard deviation) or associated estimates of uncertainty (e.g. confidence intervals)
☒	☐ For null hypothesis testing, the test statistic (e.g. *F*, *t*, *r*) with confidence intervals, effect sizes, degrees of freedom and *P* value noted *Give P values as exact values whenever suitable.*
☒	☐ For Bayesian analysis, information on the choice of priors and Markov chain Monte Carlo settings
☒	☐ For hierarchical and complex designs, identification of the appropriate level for tests and full reporting of outcomes
☒	☐ Estimates of effect sizes (e.g. Cohen's *d*, Pearson's *r*), indicating how they were calculated

Our web collection on statistics for biologists contains articles on many of the points above.

Software and code

Policy information about availability of computer code

Data collection	CaseViewer v2.4
Data analysis	R v4.5; cellranger 3.1.0, Seurat 4.1.1; Harmony 1.2.3; SingleR 2.10.1; AUCell 1.30.1; GSEA 4.4.0 SPSS v24.0; GraphPad Prism v8.0; FlowJo v10.0; ImageJ v1.54; PASS v11

For manuscripts utilizing custom algorithms or software that are central to the research but not yet described in published literature, software must be made available to editors and reviewers. We strongly encourage code deposition in a community repository (e.g. GitHub). See the Nature Portfolio guidelines for submitting code & software for further information.

Data

Policy information about availability of data

All manuscripts must include a data availability statement. This statement should provide the following information, where applicable:

- Accession codes, unique identifiers, or web links for publicly available datasets
- A description of any restrictions on data availability
- For clinical datasets or third party data, please ensure that the statement adheres to our policy

Raw sequencing data have been deposited in the Genome Sequence Archive of the National Genomics Data Center (Beijing, China) under HRA009819, HRA002792, and CRA026219. The data deposited and made public are compliant with the regulations of the Ministry of Science and Technology of China.

De-identified individual participant-level efficacy and immune monitoring data underlying the main findings, together with the study protocol, statistical analysis plan and data dictionary, are provided in Supplementary materials. Additional de-identified participant-level data not included in the Article may be made available to qualified academic investigators for non-commercial research purposes, subject to institutional review and applicable ethical and legal requirements. Requests should be directed to the corresponding author at zhanglei1@ihcams.ac.cn and will be reviewed within 4 weeks. Approved requests may require a data access agreement. Source data are provided with this paper.

Research involving human participants, their data, or biological material

Policy information about studies with human participants or human data. See also policy information about sex, gender (identity/presentation), and sexual orientation and race, ethnicity and racism.

Reporting on sex and gender	Sex was considered in the study design and recruitment to promote balanced representation across study groups. Participant sex (a biological variable) was recorded as male or female from medical records at enrollment and was not based on self-reported gender identity. An exception was the human spleen-based analyses, for which trauma spleen controls were very limited and all available control samples were from male donors; therefore, sex matching was not fully achieved for these experiments. No sex-stratified analyses were prespecified or performed because the study was not powered for sex-based comparisons.
Reporting on race, ethnicity, or other socially relevant groupings	No data on race, ethnicity, or other socially relevant groupings were collected or analyzed in this study.
Population characteristics	The study comprised four complementary human components in adults with primary ITP and controls, including a retrospective anti-CD38 mAb cohort (n = 21 ITP), a retrospective anti-CD38 mAb retreatment cohort in relapsed patients(n= 3 ITP), a prospective phase 1–2 NMN trial (n = 25 ITP), and translational mechanistic studies using spleen tissue, paired peripheral blood samples collected before and after anti-CD38 mAb therapy for single-cell RNA sequencing, and monocyte-derived macrophages (MDMs) from patients with ITP and non-ITP controls (ITP: n = 57; non-ITP controls: n=55). In addition 18 normal controls recruited for platelet aggregation and activation. Participant characteristics included age, sex, diagnostic history and prior treatments. Detailed demographic and clinical information is provided in Table 1 and Extended Data Table 3.
Recruitment	Participants received no financial compensation. Participants were recruited at a single center from patients who presented for diagnosis or treatment during the study period. Eligible individuals who met the prespecified inclusion criteria and provided written informed consent were enrolled for the prospective trial and sample collection, whereas retrospective anti-CD38 mAb cohorts were identified from clinical records. Potential biases include the single-center design, eligibility restrictions, and self-selection among patients willing and able to participate in the prospective trial. In addition, the most refractory, high-bleeding-risk patients with severe thrombocytopenia were not enrolled for ethical and safety reasons. These factors may limit the generalizability of the findings, particularly to more difficult-to-treat ITP populations.
Ethics oversight	The study was approved by the Ethics Committee of the Institute of Hematology and Blood Diseases Hospital, and all participants provided written informed consent.

Note that full information on the approval of the study protocol must also be provided in the manuscript.

Field-specific reporting

Please select the one below that is the best fit for your research. If you are not sure, read the appropriate sections before making your selection.

☒ Life sciences ☐ Behavioural & social sciences ☐ Ecological, evolutionary & environmental sciences

For a reference copy of the document with all sections, see nature.com/documents/nr-reporting-summary-flat.pdf

Life sciences study design

All studies must disclose on these points even when the disclosure is negative.

Sample size	No formal sample size calculation was performed for the mechanistic studies, which were exploratory in nature. Sample sizes for these experiments were determined on the basis of prior literature, sample availability and feasibility, particularly for patient-derived materials such as spleen tissue and peripheral blood samples. For animal experiments, group sizes were chosen to be consistent with commonly used sample sizes in the field and were considered sufficient to detect robust and reproducible effects across independent experiments. For sequencing studies and experiments involving patient-derived samples, all available eligible samples collected during the study period were included where feasible. Exact n values for each experiment are provided in the corresponding figure legends. Mouse in vivo experiments were independently repeated to confirm reproducibility. For the investigator-initiated clinical trial, sample size estimation was performed using PASS v11. Assuming that the proportion of patients achieving a platelet count ≥50 × 10^9/L within 8 weeks after treatment would be 55%, with a target value of 20% and a two-sided type I error of 0.05, 16 subjects were estimated to provide 85.6% power to test the hypothesis that the efficacy endpoint exceeds the target value. Allowing for an anticipated dropout rate of 20%, 20 patients were planned for enrolment.
Data exclusions	No data were excluded from the analyses; all collected data points/samples were included.
Replication	For sequencing data and experiments involving patient-derived samples, biological replicates from independent individuals were used. For

Replication	mouse in vivo studies, experiments were independently repeated at least twice with similar results. All attempts at replication were successful, and we did not identify any findings that could not be reproduced.
Randomization	For animal experiments, age- and sex-matched mice were used. Mice were randomly assigned to experimental groups, with animals from the same cage distributed across different treatment groups to minimize potential cage effects. The clinical trial was a single-arm study and therefore did not involve randomization.
Blinding	Blinding was not performed during data collection or analysis. Most outcomes were based on objective, instrument-derived readouts (for example, platelet counts, flow cytometry quantification and ELISA measurements), which minimized subjective assessment.

Reporting for specific materials, systems and methods

We require information from authors about some types of materials, experimental systems and methods used in many studies. Here, indicate whether each material, system or method listed is relevant to your study. If you are not sure if a list item applies to your research, read the appropriate section before selecting a response.

Materials & experimental systems

n/a	Involved in the study
☐	☒ Antibodies
☐	☐ Eukaryotic cell lines
☐	☐ Palaeontology and archaeology
☐	☒ Animals and other organisms
☐	☒ Clinical data
☐	☐ Dual use research of concern
☐	☐ Plants

Methods

n/a	Involved in the study
☐	☐ ChIP-seq
☐	☒ Flow cytometry
☐	☐ MRI-based neuroimaging

Antibodies

Antibodies used

Anti-mouse CD41 (clone MWReg30) BioLegend Cat# 133902, used for passive ITP induction, 68 µg/kg initially with escalating doses as described in Methods;
Anti-mouse CD19 (clone 1D3) BioXCell Cat# BE0150, 500 µg per mouse;
Anti-mouse CD4 (clone GK1.5) BioXCell Cat# BE0003, 200 µg per mouse;
Anti-mouse CD8 (clone 2.43) BioXCell Cat# BE0061, 200 µg per mouse;
Anti-mouse Ly6G (clone 1A8) BioXCell Cat# BE0075-1, 100 µg on day −1 and 50 µg on days +1 and +3;
Anti-Asialo-GM1 (Clone Poly21460) BioLegend Cat# 146002, 50 µL per mouse;
Anti-human CD41 (clone HIP8) BioLegend Cat# 303702, 5 µg/mL;
Anti-mouse/human CD11b-PE-Cy7(clone M1/70) BioLegend Cat# 101216, used for flow cytometry, 5 µL per test;
Anti-mouse F4/80-APC (clone BM8) BioLegend Cat# 123116, used for flow cytometry, 5 µL per test
Anti-mouse CD86-BV510 (clone GL-1) BioLegend Cat# 105040, used for flow cytometry, 5 µL per test;
Anti-mouse CD206-PE (clone C068C2) BioLegend Cat# 141706, used for flow cytometry, 5 µL per test;
Anti-human CD68-APC (clone Y1/82A) BioLegend Cat# 333810, used for flow cytometry, 5 µL per test;
Anti-human CD86-BV510 (clone IT2.2) BioLegend Cat# 305432, used for flow cytometry, 5 µL per test;
Anti-human CD206-PE (clone 15-2) BioLegend Cat# 321106, used for flow cytometry, 5 µL per test;
Anti-human CD19-FITC (clone HIB19) BioLegend Cat# 302205, used for flow cytometry, 5 µL per test;
Anti-human CD27-BV421 (clone M-T271) BioLegend Cat# 356417, used for flow cytometry, 5 µL per test;
Anti-human CD138-APC-Cy7 (clone MI15) BioLegend Cat# 356527, used for flow cytometry, 5 µL per test;
Anti-human IgD-PE-Cy7 (clone W18340F) BioLegend Cat# 307811, used for flow cytometry, 5 µL per test;
Anti-mouse CD19-FITC (clone 1D3/CD19) BioLegend Cat# 152403, used for flow cytometry, 5 µL per test;
Anti-mouse CD138-BV510 (clone 281-2) BioLegend Cat# 142521, used for flow cytometry, 5 µL per test;
Anti-mouse IgD-PE (clone 11-26c.2a) BioLegend Cat# 405705, used for flow cytometry, 5 µL per test;
Anti-mouse CD64-BV421(Clone X54-5/7.1)BiolegendCat#139309, used for flow cytometry, 5 µL per test;
Anti-human CD64-BV421(Clone 10.1)BiolegendCat#305020, used for flow cytometry, 5 µL per test;
Anti-mouse B220-FITC (clone RA3-6B2) BiolegnedCat#103205, used for flow cytometry, 5 µL per test;
Anti-mouse GL7-APC (clone GL7) BiolegnedCat#144617, used for flow cytometry, 5 µL per test;
Anti-mouse Fas-PE (clone SA367H8) BiolegnedCat#152607, used for flow cytometry, 5 µL per test;
Anti-mouse CD38-FITC (clone 90) Biolegend 102705, used for flow cytometry, 5 µL per test;
Anti-human CD38-PE (clone HIT2) Biolegend 303506, used for flow cytometry, 5 µL per test;
Anti-human CD86-PE-cy7 (clone IT2.2) Biolegend 305422, used for flow cytometry, 5 µL per test;
Anti-human CD14-APC (clone M5E2) Biolegend 301807, used for flow cytometry, 5 µL per test;
Anti-human CD42b-PE (clone HIP1) Biolegend 303906, used for flow cytometry, 5 µL per test;
Anti-human CD62P-APC-cy7 (clone AK4) Biolegend 304944, used for flow cytometry, 5 µL per test;
Anti-mouse CD41-FITC (clone MWReg30) Biolegend 133903, used for flow cytometry, 5 µL per test;
Anti-mouse CD62P (clone RMP-1) Biolegend 148303, used for flow cytometry, 5 µL per test.
Anti-human CD38 (CM313) Keymed Biosciences, 2 µg/mL
Anti-NF-κB p65 (clone D14E12) CST Cat# 8242S, 1:500
Anti-phospho-NF-κB p65 (Ser536) CST Cat# 3031S, 1:500
β-actin (clone 3H6G5) Servicebio Cat# GB12001, 1:3000
Anti-mouse CD38 (clone EPR21079) Abcam Cat# ab216343, 1:2000;
Anti-human CD38 (clone EPR4106) Abcam Cat# ab108403, 1:2000;

Anti-iNOS Ab (clone RM1017) Abcam Cat# ab283655, 1:200/1:1000;
Anti-CD163 Ab (clone EPR19518) Abcam Cat# ab182422, 1:4000;
Anti-human CD68 (clone C68/684) Abcam Cat# ab201340, 1:100;
Anti-mouse F4/80 (clone D2S9R) CST Cat# 70076, 1:8000;
HRP-conjugated goat anti-rabbit IgG Abcam Cat# ab205718, 1:4000;
Donkey anti-mouse IgG (H+L) highly cross-adsorbed secondary antibody, Alexa Fluor™ Plus 555, Thermo Fisher Cat# A32773 1:500;
Donkey anti-rabbit IgG (H+L) highly cross-adsorbed secondary antibody, Alexa Fluor 488, Thermo Fisher Cat# A21206, 1:400;

Validation

All other primary antibodies were commercially sourced and are listed in the manuscript and Reporting Summary with supplier, catalog number, clone and application. Validation information was based on the manufacturers' datasheets/websites for the indicated species and applications. For the anti-human CD38 antibody (CM313, Keymed Biosciences), validation was additionally supported by prior published use in human samples, as reported in Frontiers in Immunology (2024, 15:1410457).

Eukaryotic cell lines

Policy information about cell lines and Sex and Gender in Research

Cell line source(s)	*State the source of each cell line used and the sex of all primary cell lines and cells derived from human participants or vertebrate models.*
Authentication	*Describe the authentication procedures for each cell line used OR declare that none of the cell lines used were authenticated.*
Mycoplasma contamination	*Confirm that all cell lines tested negative for mycoplasma contamination OR describe the results of the testing for mycoplasma contamination OR declare that the cell lines were not tested for mycoplasma contamination.*
Commonly misidentified lines (See ICLAC register)	*Name any commonly misidentified cell lines used in the study and provide a rationale for their use.*

Palaeontology and Archaeology

Specimen provenance	*Provide provenance information for specimens and describe permits that were obtained for the work (including the name of the issuing authority, the date of issue, and any identifying information). Permits should encompass collection and, where applicable, export.*
Specimen deposition	*Indicate where the specimens have been deposited to permit free access by other researchers.*
Dating methods	*If new dates are provided, describe how they were obtained (e.g. collection, storage, sample pretreatment and measurement), where they were obtained (i.e. lab name), the calibration program and the protocol for quality assurance OR state that no new dates are provided.*

☐ Tick this box to confirm that the raw and calibrated dates are available in the paper or in Supplementary Information.

Ethics oversight	*Identify the organization(s) that approved or provided guidance on the study protocol, OR state that no ethical approval or guidance was required and explain why not.*

Note that full information on the approval of the study protocol must also be provided in the manuscript.

Animals and other research organisms

Policy information about studies involving animals; ARRIVE guidelines recommended for reporting animal research, and Sex and Gender in Research

Laboratory animals	BALB/c and C57BL/6J (CD45.2) mice were purchased from Beijing HFK Bioscience Co., Ltd. (Beijing, China). CD45.1 congenic mice (B6.SJL-Ptprca Pepcb/BoyJ; stock no. 002014) were obtained from The Jackson Laboratory (Bar Harbor, ME, USA). CD38 knockout mice (CD38–/–; C57BL/6Smoc-CD38em2Smoc, CD45.2; stock no. NM-KO-226125) on a C57BL/6J background were purchased from Shanghai Model Organisms Center, Inc. (Shanghai, China). For myeloid-specific deletion of CD38, Lyz2-iCre mice (C57BL/6JGpt-Lyz2em1Cin(iCre)/Gpt; stock no. T003822) and CD38-flox mice (C57BL/6JGpt-Cd38em1Cflox/Gpt; stock no. T009317) were purchased from GemPharmatech (Nanjing, China) and crossed to generate CD38fl/fl;Lyz2-iCre+ mice (myeloid-specific CD38 conditional knockout) and CD38fl/fl;Lyz2-iCre– littermate controls. All animals were housed under standard conditions, with controlled temperature (~25°C), relative humidity of 40-70%, and a 14-hour light/10-hour dark cycle. passive ITP model: BALB/c mice, 8–10 weeks old; immune cell depletion studies: BALB/c mice, 8–10 weeks old; NMN / 78c pharmacological intervention studies: BALB/c mice, 8–10 weeks old; CD38KO experiments: CD38KO mice and WT controls on a C57BL/6J background, 8–10 weeks old; bone marrow transplantation: CD45.1 recipients and WT/CD38KO donor mice on a C57BL/6J background, 8–10 weeks old myeloid-specific deletion experiments: CD38fl/fl;Lyz2-iCre+ mice and CD38fl/fl;Lyz2-iCre– littermate controls on a C57BL/6J background, 8–10 weeks old
Wild animals	The study did not involve wild animals.

Reporting on sex	For each experimental batch, the sex ratio of mice was approximately balanced across treatment groups. No sex-specific analyses were performed.
Field-collected samples	Not applicable.
Ethics oversight	The Institutional Animal Care and Use Committee (IACUC) of the Institute of Hematology and Blood Disease Hospital, Chinese Academy of Medical Sciences (CAMS).

Note that full information on the approval of the study protocol must also be provided in the manuscript.

Clinical data

Policy information about clinical studies

All manuscripts should comply with the ICMJE guidelines for publication of clinical research and a completed CONSORT checklist must be included with all submissions.

Clinical trial registration	ClinicalTrials.gov, NCT06776510
Study protocol	The full trial protocol and the statistical analysis plan are available in the Supplementary Information.
Data collection	For the prospective NMN trial, adults with primary ITP who met the prespecified eligibility criteria and provided written informed consent were enrolled during the study period. This was a single-center, open-label, interventional study conducted at a tertiary academic hospital in China. Participants were enrolled between January 15, 2025 and March 17, 2025. Clinical data, including laboratory values, treatment administration, and safety outcomes, were collected from January 2025 through July 2025. Data collection was performed by trained study personnel using standardized case report forms and entered into a secure electronic data capture system. Platelet counts and safety labs were assessed in a central clinical laboratory. For the retrospective anti-CD38 mAb cohorts, eligible patients were identified from clinical records according to predefined inclusion and exclusion criteria. Potential biases include the single-center design, the limited sample size, eligibility restrictions, and self-selection among patients willing and able to participate in the prospective trial. Ethical and safety considerations precluded enrolment of the most refractory, high-bleeding-risk patients with severe thrombocytopenia, and enrolled patients had relatively higher baseline platelet counts. These factors may limit the generalizability of the findings, particularly to more difficult-to-treat ITP populations. However, key efficacy and safety endpoints were based on objective laboratory and clinical assessments.
Outcomes	The primary endpoints were prespecified in the study protocol and statistical analysis plan before study initiation and comprised: (1) safety and tolerability, assessed by the incidence and severity of treatment-emergent adverse events (AEs) and serious AEs (SAEs) together with routine laboratory tests, with severity graded according to CTCAE v5.0; and (2) efficacy, defined as the proportion of patients achieving a platelet count ≥50 × 10^9/L within 2 weeks of treatment initiation, confirmed by two consecutive measurements at least 1 day apart, in the absence of rescue therapy and without any dose increase of TPO-RAs or corticosteroids during the study period. Platelet counts were measured using automated hematology analyzers in a central clinical laboratory. Secondary endpoints were also prespecified and included (1) the proportion of patients with platelet count ≥50 X 10^9/L at each scheduled visit (week 1, 2, 3, 4, 6 and 8); (2) time to platelet count ≥30 X 10^9/L (with at least a two-fold increase from baseline) and to ≥50 X 10^9/L; (3) platelet counts at each scheduled visit; (4) the proportion of patients receiving emergency (rescue) treatment within 2 weeks and over the entire study period; (5) cumulative weeks with platelet count ≥30 X 10^9/L and ≥50 X 10^9/L during the 8-week study period; (6) change in bleeding score from baseline to week 2 assessed by the WHO bleeding scale; (7) the proportion of patients achieving platelet counts ≥50 X 10^9/L at least once within the first 4 weeks; (8) partial response (PR) rate within 4 weeks; and (9) the proportion of suboptimal response (SR) at each scheduled visit. Platelet counts were measured using automated hematology analyzers in a central clinical laboratory. Bleeding was assessed using the WHO bleeding scale. To more comprehensively assess treatment efficacy, we predefined modified response categories for ITP. Complete response (CR) was defined as a post-treatment platelet count ≥100 × 10^9/L without bleeding, confirmed by at least two assessments performed ≥7 days apart. Partial response (PR) was defined as a platelet count ≥30 × 10^9/L and <100 × 10^9/L, with a ≥2-fold increase from the baseline platelet count and no bleeding, confirmed by at least two assessments ≥7 days apart. Suboptimal response (SR) was defined as a platelet count ≥30 × 10^9/L with a ≥1.5-fold but <2-fold increase from baseline and no bleeding, confirmed by at least two platelet count measurements taken ≥7 days apart. No response (NR) was defined as failure to meet the criteria for CR, PR or SR. Relapse was defined as any of the following after an initial response: a platelet count <30 × 10^9/L, or <1.5-fold increase from baseline, or the occurrence of clinical bleeding. CR, PR and SR required confirmation by at least two platelet measurements obtained ≥7 days apart; NR and relapse required confirmation by at least two assessments performed ≥1 day apart.

Dual use research of concern

Policy information about dual use research of concern

Hazards

Could the accidental, deliberate or reckless misuse of agents or technologies generated in the work, or the application of information presented in the manuscript, pose a threat to:

No	Yes	
☐	☐	Public health
☐	☐	National security
☐	☐	Crops and/or livestock
☐	☐	Ecosystems
☐	☐	Any other significant area

Experiments of concern

Does the work involve any of these experiments of concern:

No	Yes	
☐	☐	Demonstrate how to render a vaccine ineffective
☐	☐	Confer resistance to therapeutically useful antibiotics or antiviral agents
☐	☐	Enhance the virulence of a pathogen or render a nonpathogen virulent
☐	☐	Increase transmissibility of a pathogen
☐	☐	Alter the host range of a pathogen
☐	☐	Enable evasion of diagnostic/detection modalities
☐	☐	Enable the weaponization of a biological agent or toxin
☐	☐	Any other potentially harmful combination of experiments and agents

Plants

Seed stocks	*Report on the source of all seed stocks or other plant material used. If applicable, state the seed stock centre and catalogue number. If plant specimens were collected from the field, describe the collection location, date and sampling procedures.*
Novel plant genotypes	*Describe the methods by which all novel plant genotypes were produced. This includes those generated by transgenic approaches, gene editing, chemical/radiation-based mutagenesis and hybridization. For transgenic lines, describe the transformation method, the number of independent lines analyzed and the generation upon which experiments were performed. For gene-edited lines, describe the editor used, the endogenous sequence targeted for editing, the targeting guide RNA sequence (if applicable) and how the editor was applied.*
Authentication	*Describe any authentication procedures for each seed stock used or novel genotype generated. Describe any experiments used to assess the effect of a mutation and, where applicable, how potential secondary effects (e.g. second site T-DNA insertions, mosiacism, off-target gene editing) were examined.*

ChIP-seq

Data deposition

☐ Confirm that both raw and final processed data have been deposited in a public database such as GEO.

☐ Confirm that you have deposited or provided access to graph files (e.g. BED files) for the called peaks.

Data access links *May remain private before publication.*	*For "Initial submission" or "Revised version" documents, provide reviewer access links. For your "Final submission" document, provide a link to the deposited data.*
Files in database submission	*Provide a list of all files available in the database submission.*
Genome browser session (e.g. UCSC)	*Provide a link to an anonymized genome browser session for "Initial submission" and "Revised version" documents only, to enable peer review. Write "no longer applicable" for "Final submission" documents.*

Methodology

Replicates	*Describe the experimental replicates, specifying number, type and replicate agreement.*
Sequencing depth	*Describe the sequencing depth for each experiment, providing the total number of reads, uniquely mapped reads, length of reads and whether they were paired- or single-end.*
Antibodies	*Describe the antibodies used for the ChIP-seq experiments; as applicable, provide supplier name, catalog number, clone name, and lot number.*
Peak calling parameters	*Specify the command line program and parameters used for read mapping and peak calling, including the ChIP, control and index files used.*

Data quality	*Describe the methods used to ensure data quality in full detail, including how many peaks are at FDR 5% and above 5-fold enrichment.*
Software	*Describe the software used to collect and analyze the ChIP-seq data. For custom code that has been deposited into a community repository, provide accession details.*

Flow Cytometry

Plots

Confirm that:

☒ The axis labels state the marker and fluorochrome used (e.g. CD4-FITC).

☒ The axis scales are clearly visible. Include numbers along axes only for bottom left plot of group (a 'group' is an analysis of identical markers).

☒ All plots are contour plots with outliers or pseudocolor plots.

☒ A numerical value for number of cells or percentage (with statistics) is provided.

Methodology

Sample preparation	Single-cell suspensions were prepared separately for mouse and human flow cytometry experiments. Mouse samples. For splenic immune profiling (including macrophage polarization and B cell subsets such as plasma cells and germinal center B cells), spleens were processed into single-cell suspensions and adjusted to 2e7 cells/mL; 100 µL was used per staining tube. For BMDM-based assays (macrophage polarization, FcγRI expression and platelet phagocytosis), bone marrow-derived macrophages were detached with Accutase after the indicated treatments to generate single-cell suspensions (3e6 cells/mL; 100 µL per tube). For quantification of violet-labelled platelets in mouse plasma, peripheral blood was centrifuged at 200g for 10 min to obtain platelet-rich plasma (PRP), and 10 µL plasma was used for analysis. For mouse platelet activation assays, 100 µL of PRP diluted with modified Tyrode's buffer to a platelet concentration of 2e8/mL was pretreated with NMN for 30 min and then stimulated with collagen for 5 min, followed by flow cytometric staining for FACS analysis. Human samples. For immunophenotyping of peripheral blood B cell and monocyte subsets before or after NMN treatment, 100 µL whole blood was used per tube. For MDM-based assays (macrophage polarization, FcγRI expression and platelet phagocytosis), monocyte-derived macrophages were detached with Accutase after the indicated treatments to generate single-cell suspensions (3e6 cells/mL; 100 µL per tube). For human platelet activation assays, 100 µL of PRP adjusted to a platelet concentration of 2e8/mL was pretreated with NMN for 30 min and then stimulated with collagen for 5 min, followed by flow cytometric staining for FACS analysis.
Instrument	BD FACSCanto II and FongCyte
Software	FlowJo v10.0 TreeStar
Cell population abundance	The abundance of each cell population was determined by calculating the percentage of marker-positive cells. Data are presented as percentages. No cell sorting was performed in this study, and therefore post-sort purity was not assessed.
Gating strategy	FSC/SSC scatter gating was first applied to define the starting cell population. For CD38 expression on splenic macrophage polarization , target cell population were gated as F4/80+CD11blow. For mouse splenic macrophage polarization , target cell population was gated as F4/80+CD11blowCD86+CD206- (M1) and F4/80+CD11blowCD86-CD206+ (M2) For macrophage polarization of BMDM and MDM, target cell population were gated as F4/80+CD86+CD206- or CD68+CD86+CD206-(M1) and F4/80+CD86-CD206+ or CD68+CD86-CD206+ (M2) For platelet phagocytosis of BMDM and MDM, target cell population were gated as F4/80+CFSE+ or CD68+CFSE+ For platelet phagocytosis in vivo, target cell population were gated as violet+. For B subset detect in mouse spleen, plasma cells were gated as CD19+IgD-CD138+. For B subset in Peripheral blood from patients,naive B cell population was gated as CD19+IgD+CD27-, class-unswitched memory cells were gated as CD19+IgD+CD27+, and class-switched memory cells were gated as CD19+IgD-CD27+, plasmablasts were gated as CD19+CD27+CD138+. For GC subset detect in mouse spleen, GC cells were gated as B220+FAS+GL7+. For CD38, CD86 and CD206 expression (MFI) on monocytes in Peripheral blood from patients, monocytes were gated as CD14+. For CD62P expression (MFI) on platelets in plasma, mouse platelets were gated as CD41+, human platelets were gated as CD42b+. The specific gating strategy is provided in the supplementary materials.

☒ Tick this box to confirm that a figure exemplifying the gating strategy is provided in the Supplementary Information.

Magnetic resonance imaging

Experimental design

Design type	*Indicate task or resting state; event-related or block design.*

Design specifications

Specify the number of blocks, trials or experimental units per session and/or subject, and specify the length of each trial or block (if trials are blocked) and interval between trials.

Behavioral performance measures

State number and/or type of variables recorded (e.g. correct button press, response time) and what statistics were used to establish that the subjects were performing the task as expected (e.g. mean, range, and/or standard deviation across subjects).

Acquisition

Imaging type(s)

Specify: functional, structural, diffusion, perfusion.

Field strength

Specify in Tesla

Sequence & imaging parameters

Specify the pulse sequence type (gradient echo, spin echo, etc.), imaging type (EPI, spiral, etc.), field of view, matrix size, slice thickness, orientation and TE/TR/flip angle.

Area of acquisition

State whether a whole brain scan was used OR define the area of acquisition, describing how the region was determined.

Diffusion MRI ☐ Used ☐ Not used

Preprocessing

Preprocessing software

Provide detail on software version and revision number and on specific parameters (model/functions, brain extraction, segmentation, smoothing kernel size, etc.).

Normalization

If data were normalized/standardized, describe the approach(es): specify linear or non-linear and define image types used for transformation OR indicate that data were not normalized and explain rationale for lack of normalization.

Normalization template

Describe the template used for normalization/transformation, specifying subject space or group standardized space (e.g. original Talairach, MNI305, ICBM152) OR indicate that the data were not normalized.

Noise and artifact removal

Describe your procedure(s) for artifact and structured noise removal, specifying motion parameters, tissue signals and physiological signals (heart rate, respiration).

Volume censoring

Define your software and/or method and criteria for volume censoring, and state the extent of such censoring.

Statistical modeling & inference

Model type and settings

Specify type (mass univariate, multivariate, RSA, predictive, etc.) and describe essential details of the model at the first and second levels (e.g. fixed, random or mixed effects; drift or auto-correlation).

Effect(s) tested

Define precise effect in terms of the task or stimulus conditions instead of psychological concepts and indicate whether ANOVA or factorial designs were used.

Specify type of analysis: ☐ Whole brain ☐ ROI-based ☐ Both

Statistic type for inference

Specify voxel-wise or cluster-wise and report all relevant parameters for cluster-wise methods.

(See Eklund et al. 2016)

Correction

Describe the type of correction and how it is obtained for multiple comparisons (e.g. FWE, FDR, permutation or Monte Carlo).

Models & analysis

n/a	Involved in the study
☐	☐ Functional and/or effective connectivity
☐	☐ Graph analysis
☐	☐ Multivariate modeling or predictive analysis

Functional and/or effective connectivity

Report the measures of dependence used and the model details (e.g. Pearson correlation, partial correlation, mutual information).

Graph analysis

Report the dependent variable and connectivity measure, specifying weighted graph or binarized graph, subject- or group-level, and the global and/or node summaries used (e.g. clustering coefficient, efficiency, etc.).

Multivariate modeling and predictive analysis

Specify independent variables, features extraction and dimension reduction, model, training and evaluation metrics.